TECHNO-ECONOMICS ON THE APPLICATION OF HYDRAULICS IN WIND TURBINE DRIVE-TRAINS & THE DEVELOPMENT OF INTEGRATED RENEWABLE ENERGY SYSTEMS FOR USE IN WATER SECURITY ALONG THE US-MEXICO BORDER

by

Michael S. Roggenburg

A Thesis

Submitted to the Faculty of Purdue University

In Partial Fulfillment of the Requirements for the degree of

Master of Science in Mechanical Engineering

Mechanical Engineering

West Lafayette, Indiana

December 2020

THE PURDUE UNIVERSITY GRADUATE SCHOOL
STATEMENT OF COMMITTEE APPROVAL

Dr. David M. Warsinger

School of Mechanical Engineering

Dr. Luciano Castillo

School of Mechanical Engineering

Dr. Jim Braun

School of Mechanical Engineering

Approved by:

Dr. Nicole L. Key

I would like to thank all my colleagues, friends and family who supported me through the completion of these studies and my coursework. In between the satisfying moments of graduate school brought by successful tests, experiments and exams comes disappointment and long nights. Without the ability to bounce ideas off colleagues or spend a much-needed night of relaxation with friends, this experience would not have been as fulfilling. I would especially like to thank for family for supporting me during hard times when I questioned my choice of study.

ACKNOWLEDGMENTS

I would like to thank the Kenninger family for providing the resources to conduct this set of studies as well as the accompanying hydraulic test bench created by the lab group. Their continual support has made the findings of this research possible and promoted further interest in the applications of renewables and alterations to their systems.

I would like to thank Dr. Monika Ivantysynova for initiating the study of the hydraulic drivetrain for wind turbines. Unfortunately, she was unable to see the completion of this study due to a terminal fight with cancer. Her management of the Maha Fluid Power Research Center and leadership of its research interests created a collaborative environment which guided the creation of the hydraulic drivetrain test bench and provided invaluable guidance on the techno-economics of hydraulic used in the first paper presented.

I would also like to thank Dr. David M. Warsinger and Dr. Jim Braun for providing unparalleled guidance on the second study presented. Dr. Warsinger is a world class scientist researching desalination techniques and water policy/usage and provided extensive insight on the reverse osmosis technologies covered and the handling of water distribution/usage in the analysis. His assistance on formatting and writing the final journal manuscripts was also invaluable for understanding the intricacies of academic writing. Dr. Braun is a specialist in thermodynamics, HVAC and renewable applications at Purdue. His courses covered many renewable technologies in depth and provided a vital understanding of renewable energy modeling, grid integration and life-cycle emissions. Without his teaching and guidance this work would not be as detailed and industrially applicable as it became and my interest in renewables would have stopped with just wind energy.

Disclaimer of Published Work

In the following work, Chapters 2 and 3 have been recreated from papers either previously published or pending publication by the author. To avoid plagiarism, acknowledgement of these publications is presented here and accompanying references are provided.

Chapter 2: Roggenburg M, Esquivel-Puentes HA, Vacca A, Bocanegra Evans H, Garcia-Bravo JM, Warsinger DM, et al. Techno-economic analysis of a hydraulic transmission for floating offshore wind turbines. Renew Energy 2020;153:1194–204. doi:10.1016/j.renene.2020.02.060.

Chapter 3: Roggenburg M, Warsinger DM, Bocanegra Evans H, Castillo L. Combatting Water Scarcity and Economic Distress Along the US-Mexico Border Using Renewable Powered Desalination. Appl Energy (Under Rev. 2020).

TABLE OF CONTENTS

LIST OF TABLES

LIST OF FIGURES

ABSTRACT

Renewable energy adoption is critical when considering future energy grids and how they impact the environment, economy and society. While fossil fuels have traditionally been employed to generate the electricity used across every facet of the global economy, renewables are becoming increasingly more attractive as a substitute. Fossil fuels have historically outperformed their clean energy counterparts in terms of levelized cost. However, over the last few decades renewables have become extremely cost competitive and are starting to outpace their opposition as advancements in technology continue. As the cost gap between "brown" and "green" energy sources decreases, energy grid mixes will adopt more sustainably responsible generation, positively impacting the planet.

In the following thesis, two studies are presented which demonstrate new innovations for decreasing the cost of offshore wind energy and how renewables and desalination can be integrated along the US-Mexico border. The first study describes an itemized breakdown of how substituting the mechanical transmission with hydraulics can lower the life-time cost of an offshore wind turbine. The second analysis details a complex wind and solar powered clean water production and distribution network to combat ongoing water scarcity along the US-Mexico border. Both concepts push the boundaries of scientific innovation and its application for solving social and economic issues.

1. INTRODUCTION AND BACKGROUND

1.1 Thesis Scope

While physical advancements are important, techno-economic studies are becoming equally significant as these studies help identify when and where certain renewables work best and how they compare to fossil fuel. To illustrate how future renewable innovations can widen the existing cost gap with fossil fuel, an analysis is presented which evaluates the potential benefits of replacing the traditional mechanical drivetrain in an offshore wind turbine with a hydraulic version. Mass redistribution, technological redundancy and component redesigning are all considered in evaluating cost reductions. The installed and levelized costs produced by this "hydraulic" wind turbine are compared with existing global wind turbine economics to show the future savings associated with its adoption.

While sustainable electrical grids are important, clean water security is also becoming a pressing concern around the world which has yet to be effectively solved. Fortunately, these two issues can be handled in a co-dependent fashion by using renewable energy to produce clean water sustainably. A practical example of this design can be applied to the US-Mexico border which has begun to feel the impact of mismanaged water resources. This mismanagement is causing a strain on the population and industry in the region, especially on the Mexican side. A comprehensive study is presented which explored how renewables could be integrated with large-scale desalination plants to provide sustainable clean water to the area. Different types of renewables were modeled to power a set of current and future technology reverse osmosis plants. These plants provided desalinated seawater from the Pacific and/or Gulf which was pumped inland along the border using the renewable energy. The study shows the cost of water and electricity that can be produced by employing this large-scale infrastructure along the US-Mexico border and details the social and economic benefits that can be gained from using renewables over fossil fuel. The results aim to provide a starting concept to help develop long term water security in the region.

1.2 Global Emissions: A Bleak Present but Promising Future

The global emission of greenhouse gases has reached record levels. Since the start of the industrial age, humans have increased atmospheric CO2 concentration from ~280 ppm to over 400

ppm at an exponential rate of ~0.17% per year[1–3]. This massive accumulation of CO2 and its equivalents, largely caused by the burning of fossil fuels and deforestation, inhibit Earth's ability to shed heat[4].

Global warming and climate change are an outcome of these emissions that many scientists agree will cause unprecedented negative consequences for humanity[5]. Temperatures will elevate and become more erratic, destroying entire ecosystems and food chains[6]. Seasonal natural disasters, such as hurricanes and monsoons, will become more commonplace[7]. Sea-levels will rise, redrawing coastlines and forcing human migration in the hundreds of millions[8–10].

However, the world will not let this conclusion occur without a valiant fight. Global policymakers, captains of industry and everyday members of society are now rallying against this common threat. Decarbonization of the transportation sector in the form of electric and fuel cell vehicles as well as the adoption of renewables for low-carbon heat and power production are some of the ways this war can be fought[11]. Although there are decades if not centuries of environmental irresponsibility to undo, the path to victory is becoming clearer every day.

1.3 Global Economic Trends in Renewable Energy

Renewable energy has proliferated on a global scale as countries strive to become more carbon neutral, especially following the widespread adoption of the Kyoto Protocol and Paris Climate Agreement[12,13]. In the ongoing war against climate change, decarbonizing the power sector has become a key battleground in offsetting air pollution. Roughly 25% of global emissions originate in this sector and renewable energy is the most significant avenue for reducing its contribution[11].

Unfortunately, price competition with fossil fuel presents a difficult hurdle for emerging green energy technologies. For many years following the initial UN conventions on climate change countries continued to deploy fossil fuel plants, knowing their negative impacts. This was largely influenced by the price disparity between developing renewables and established fossil fuel. In recent years the conversation has changed though. Shown in Figure 1-1, the global cost of renewables has drastically declined so that traditional renewables are now entirely cost competitive with fossil fuels[14].

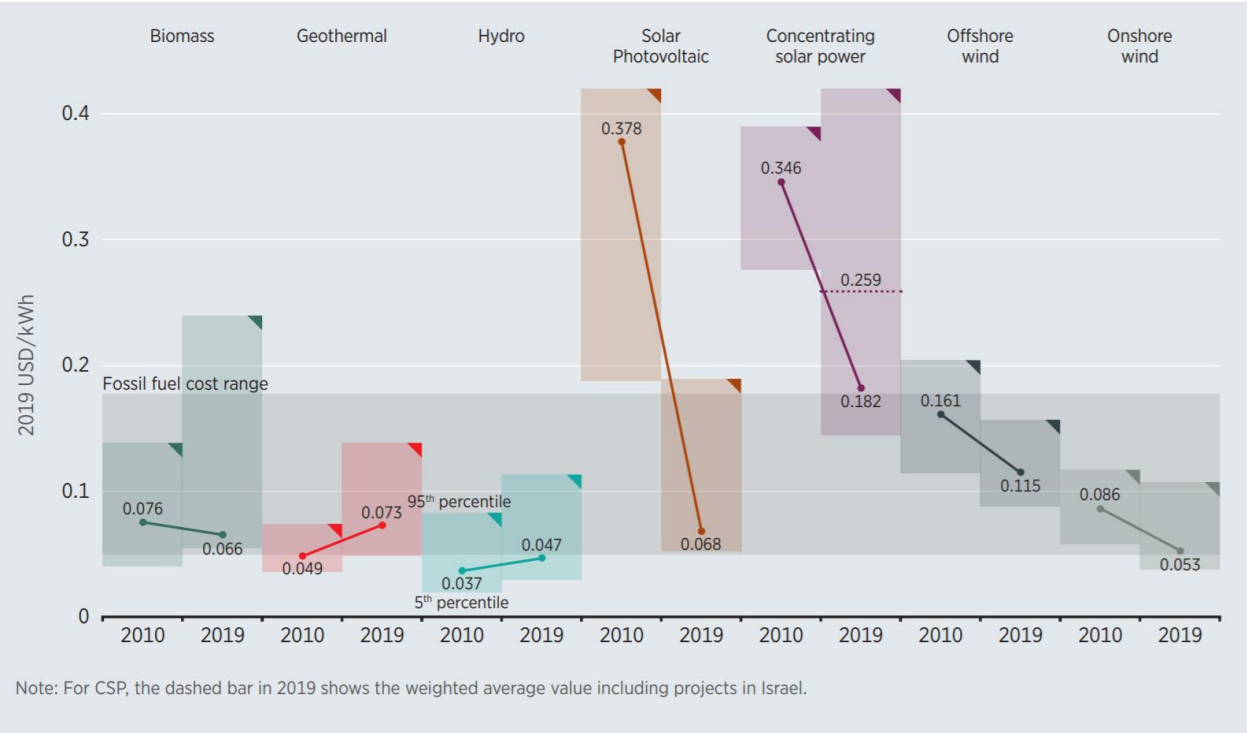

Figure 1-1: Global weighted average levelized cost of electricity from utility-scale renewable power generation technologies, 2010 to 2019 (taken from IRENA)[14].

In terms of levelized costs during the period from 2010-19, solar PV has seen the greatest decline with an 82.0% change. Mass production, widespread adoption and technological innovation are factors that contributed to this immense drop. Concentrating Solar Power (CSP) also experienced a large decline of 47.4% but this technology has yet to see the same large-scale deployment[14]. While onshore wind has been a competitive form of energy generation for decades, having been widely adopted in Europe and North America, it still saw a decline of 38.4% and can now even outperform the cheapest fossil fuels. Offshore wind is a major resource which is being tapped across Europe and more recently in the USA[15–19]. While relatively expensive when compared to onshore wind, its placement in otherwise unusable territory and massive capacity potential make it a key player in decarbonization. The cost decrease of 28.6% makes deployment of this technology even more attractive.

Solar PV and wind turbine adoption is crucial in the fight against climate change. Their decline in price seen over this decade can be attributed in part to technological innovation. Tracking systems for solar panels and cheaper components, such as the hydraulic drivetrain presented in Chapter 2, for wind turbines are recent advances that helped produce this drop[20–

30]. Integrating and evaluating such innovations in new projects is critical to unlocking the full potential of renewables against fossil fuel.

1.4 Significance of Levelized Cost as a Comparative Metric

While both fossil fuel and renewable energy produce electricity, equating them can be like comparing apples and oranges under many circumstances. Fossil fuel is demand response oriented and requires a supply chain of non-sustainable fuel. Conversely, renewables convert resources when they are available, making them less flexible, yet require no fuel except in the case of biofuel technology. Many more differences arise when diving into greater detail. In order to accurately compare these technologies in the marketplace, a metric known as Levelized Cost of Electricity (LCOE) was developed and is widely used to gauge the economics of new projects[31–33]. The formula used for calculation takes many different forms depending on a variety of factors but is generally accepted in its simplest form as:

$$LCOE = \frac{\sum_{t=1}^{n} \frac{I_t + M_t + F_t}{(1+r)^t}}{\sum_{t=1}^{n} \frac{E_t}{(1+r)^t}} \quad (1\text{-}1)$$

Covering investment expenditures (I_t) in year t, operations and maintenance expenditures (M_t) in year t, fuel expenditures (F_t) in year t (if applicable), electricity generation (E_t) in year t, current market discount rate (r) and the economic life of the system (n).

This formula takes the total discounted cost of the system and divides it by the discounted energy produced over its lifespan. By considering the differences between the cost of building the system and maintaining it against how much energy the system produces, vastly different technologies can be compared, even globally. In the case of fossil fuels vs renewables, while fossil fuel plants are generally cheaper to build, green tech's smaller variable operation and maintenance (i.e. fuel) component evens out their costs over the system lifespan[34]. The output of this formula is also in familiar units ($/kWh), which gives developers an easy way to value of the energy produced against what they may be able to sell it for in an open market.

1.5 The Global Water Crisis

Global warming may be a major future issue for humanity to overcome, but a crisis surrounding access to clean water bears down with even more weight today. Unlike climate

change's effects which are considered in the long term, drought and overpopulation are straining the world's supply of water presently. As of 2017, ~1/3 of the world's population remains without access to sustainable drinking water, life's most basic resource[35]. Traditionally, this water comes from above-ground rivers/lakes and below-ground aquifers. Around the world and especially in developing industrial countries, these resources are being overdrawn and/or polluted, exacerbating the problem[36].

Countries such as South Africa and India have already felt the full gravity of water scarcity as entire cities, such as Cape Town, South Africa and Chennai, India, were left without access[37–41]. Fortunately, treated saltwater was exploited to fill the gap and can be used to great effect in many other problematic locations. Saltwater desalination has existed for a millennium in the form of solar stills. With technological progression, these stills evolved into complex thermal systems and finally into the apex of efficiency, reverse osmosis, or pressurized membrane desalination[42].

Only ~1.10% of the world's water is clean and accessible, with another ~2.40% trapped in ice and the remaining ~96.5% as saltwater[43]. As the population increases, Earth's available freshwater will be even less equipped to satisfy humanity's needs. Desalination technology will be critical for ensuring everyone has proper access to water by refining saltwater's essentially unlimited supply.

1.5.1 US-Mexico Implications

A specific location that has become increasingly afflicted with the water shortages is the US-Mexico border. Historically, aquifers and rivers were shared across this boundary, but these resources are becoming inadequate to sustain the region[44–47]. As society and industry continue to grow, these natural sources of water will only become more strained. Citizens in Mexico are already attempting to seize state-controlled stores of water to protect their agricultural interests[48]. If sustainable sources of water are not introduced to the region, long-term conflict will likely result. Chapter 3 presents a conceptual framework for integrating renewables and desalination to solve this growing crisis.

2. TECHNO-ECONOMIC ANALYSIS OF A HYDRAULIC TRANSMISSION FOR FLOATING OFFSHORE WIND TURBINES

2.1 Abstract

Mechanical gearboxes have one of the highest failure rates of wind turbine components while being one of the most expensive parts to replace or service. They are easily fatigued and have a low power rating relative to their size and mass. In this article, hydraulic transmissions are proposed as an alternative to mechanical drive trains and their feasibility has been established, particularly for offshore wind turbine applications. Here, we provide an in-depth analysis regarding the techno-economic benefits of replacing the mechanical gearbox with a hydraulic transmission in an offshore system. Our analysis shows that hydraulic transmissions are particularly beneficial for offshore applications: (i) relocating 35.3% of the nacelle mass to the base, thus moving the center of gravity toward the ground level, (ii) diminishing operation and maintenance costs, and (iii) replacing now-redundant power electronics. These three benefits contribute to saving between 3.92-18.8% on the Levelized Cost of Electricity for average cost offshore wind turbines.

2.2 Introduction

The wind turbine industry has seen a dramatic revolution in technological development over the last decade. This revolution has brought down the cost of energy for offshore applications by maximizing power capacity, increasing generation efficiency and minimizing installation costs [49]. Researchers have made vital efforts toward blade design and environmental cohabitation as well [50,51]. Nevertheless, offshore wind energy needs to become more cost effective to compete globally with fossil fuel power generation [34]. Major costs for offshore wind energy generation lie in the operation and maintenance (associated with repairs at high altitude) of the turbine as well as the structural design and the logistics of mobilizing maintenance personnel and equipment to an offshore location. For instance, the mechanical gearbox is one of the main cost sinks, including hard (i.e. parts) and soft (i.e. maintenance) expenses, and its large mass increases structural costs [52–55].

The hydraulic transmission design used in the analysis utilizes a coupled pump and motor system which transfer power through a set of high- and low-pressure lines (see figures 2-1,2). As a result, the output shaft can be relocated to the base of the tower [28,56]. The usage of variable displacement pumps and motors, and the integration of accumulators, allows for smoothing the input wind power profile. Significant research on the feasibility of the transmission has been conducted worldwide and its efficacy has been repeatedly validated [29,57–60]. Unfortunately, almost every major research study falls short of evaluating the full techno-economic potential of this transmission, stopping at a conceptual schematic/simulation or at most a test bench exploring physical characteristics [27,61–67]. There have been a small number of private companies that have designed fully commercial prototypes, most notably the partnership between Artemis Intelligent Power and MHI Vestas Offshore Wind [26,68–70]. However, these prototypes do not explicitly discuss the economic benefits of redesigning the turbine around a hydraulic transmission.

Our analysis assesses the economic impact of utilizing a hydraulic transmission and attempts to place a physical cost savings range on its usage for various size turbines, specifically for offshore wind generation. The objective of this study is to provide a best estimate for how this new transmission may change the underlying levelized cost economics of offshore wind turbines in comparison to traditional turbines. Early on, it was found that the majority of the financial benefits of the alteration are exclusive to offshore turbines due to their overwhelming reliance on structural design [71]. This insight led the group to focus solely on offshore wind projects and determine the mass and cost reduction benefits that may be seen through redesigning standard turbines around the new transmission.

We show that not only does the new transmission increase the power capacity of a given turbine, it also reduces the structural requirements for the tower and foundation by relocating top mass. The power rating for a hydraulic transmission is much higher than that for a mechanical drivetrain, can withstand a much longer period of wear and tear and perform at higher wind velocities [26,66]. With the use of accumulators and variable displacement pumps/motors, signal smoothing of the transferred wind energy can be achieved, eliminating the need for variable frequency electronics [64,72,73]. Furthermore, since hydraulic transmission input/output shafts are decoupled through the motor and pump via fluid lines, relocating the output of the transmission to the base will reduce the nacelle mass by about 35.3% while only adding a small fraction of this mass to the base.

The manuscript is distributed as follows: Section 2.3 details the design of the hydraulic transmission used in the turbine and describes the components evaluated. Section 2.4 defines the model turbine and details the rationale for the cost reductions accounted for in the study. Section 2.5 applies these reductions to a reference set of offshore wind turbine component mass and cost values. Section 2.6 outlines costs associated with the operation and maintenance of the turbine system. Section 2.7 describes the resolution and type of data used as well as some sensitivity considerations. Section 2.8 depicts the energy cost analysis and its results and Section 2.9 provides concluding remarks.

2.3 Model Description

2.3.1 Hydraulic Transmission Design

The design evaluated in this analysis considers the replacement of the mechanical gearbox with a fluid powered hydraulic transmission. Major benefits of the replacement include large amounts of mass relocation, smoothing of the input wind power profile, longevity of internal parts and higher power capacity [28,64–66,73–76]. The transmission will take the low speed high torque input work from the wind turbine rotor and translate it into high speed output work with a specified angular velocity. Figure 2-1 illustrates how the nacelle components are altered using a hydraulic transmission. Specifically, all parts between and including the generator and the main shaft are moved to the base, replaced only by a hydraulic pump in the nacelle.

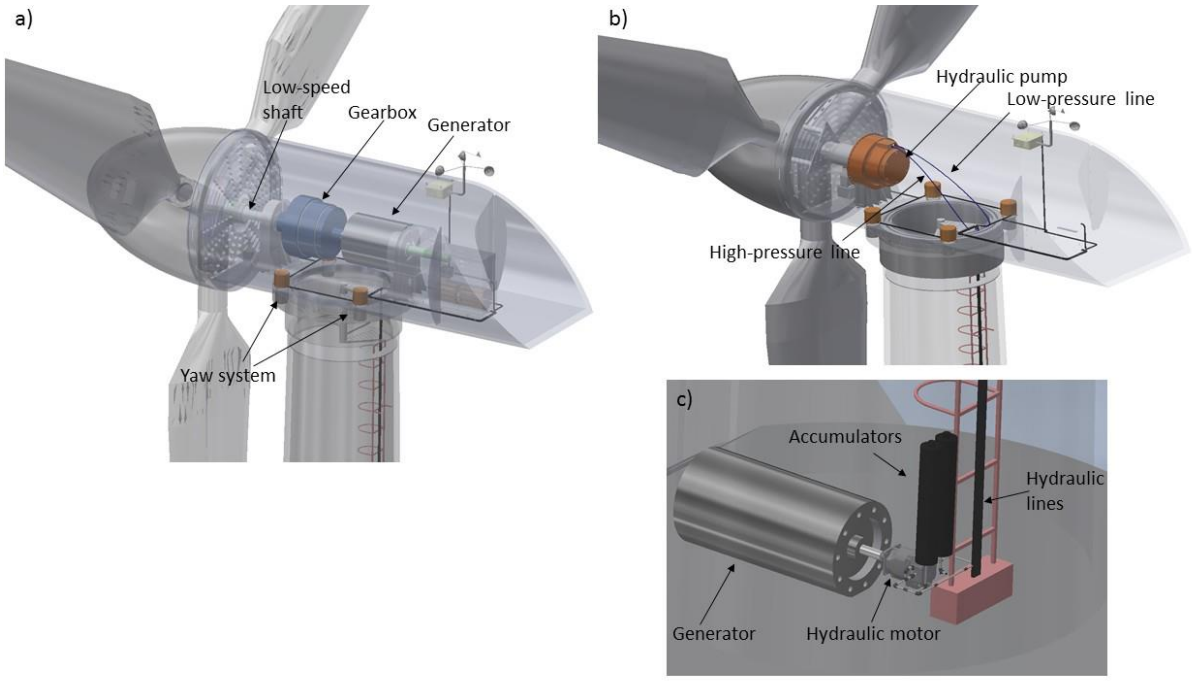

Figure 2-1: Offshore wind turbine with traditional gearbox configuration (a) vs. hydraulic transmission configuration: nacelle (b) and base (c). Observe the consolidation of parts at the base in the hydraulic configuration in comparison to the traditional gearbox where all are in the nacelle. This is meant to show the scale of mass and parts redistribution throughout the turbine caused by the transmission substitution.

The new transmission consists of an open circuit architecture for hydrostatic transmissions, including accumulators in the high-pressure line. The pump will be coupled with the low speed rotor shaft in the nacelle of the turbine and the motor is located at the base, connected by fluid transmission lines. Accumulators will be placed at the bottom near the motor and serve primarily as shock absorbers for the system.

Technology for hydrostatic transmission systems include the use of either a variable displacement pump or a variable displacement motor to allow for speed and torque regulation (or both). The simpler solution, from the controllability prospective, uses variable displacement pumps [67]. However, low speed pumps with high displacement (higher than 1000 cm3/rev) are rare in industry and predominantly fall under the category of radial piston design, which is a fixed displacement design. The only significant exception is represented by the Artemis radial piston unit, which implemented a digital displacement technology and found a pilot application in wind energy [68,70].

The hydraulic motor does not have the same low speed requirements of the pump, and therefore it can be of a lower displacement and high speed. This kind of unit can be variable displacement, which justifies the choice for the system taken as reference in this work, consisting of a fixed displacement pump, a variable displacement motor and an accumulator. The accumulator will be placed at ground level before the motor in the high-pressure line, to minimize nacelle mass and to provide the longest possible lead time to reach to pressure changes coming from the pump. The variable displacement motor varies the displacement according to the accumulator pressure, to provide an output torque that matches the wind conditions. The accumulators are one of the most important parts of the system and are used for absorbing fluctuations from the wind, smoothing the signal, and storing this energy to stabilize the system under low wind conditions.

The hydraulics industry has limited choices for the required pumps of larger transmission designs. Therefore, it is impossible to generate an overall efficiency for different turbines at this moment. In this analysis, a 3 MW offshore turbine is modelled and a 2.2MW Bosch-Rexroth Hagglunds large radial piston pump is considered and scaled accordingly. The optimal efficiency for such a pump is shown to be around 96% [77]. According to Laguna's detailed analysis, the overall efficiency of the transmission, including motor and transmission lines is estimated at 80% [26]. In addition, it is well-known that the lifespan of well-designed hydrostatic machines, particularly of the radial piston design is beyond 10 years and in some cases over 20 years, particularly for intermittent operation or operation with discontinuous loads [35,36]. This makes this technology very attractive for long term power generators.

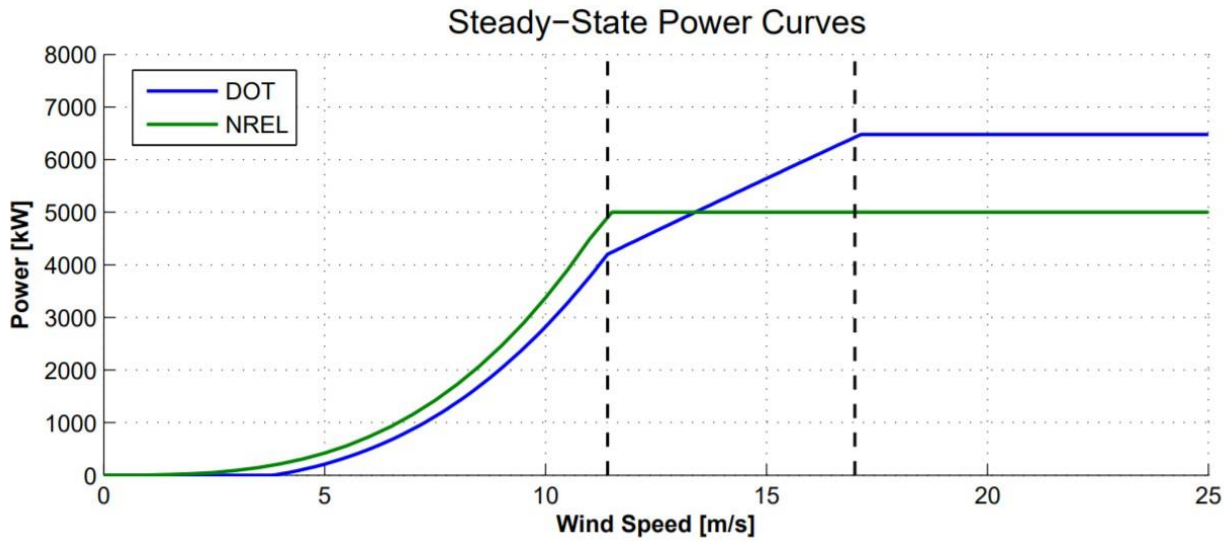

Figure 2-2: A power curve of a test bench hydraulic wind turbine developed by Delft University is shown (DOT corresponds to Delft Offshore Turbine) (Blue). The NREL 5 MW reference turbine is used as a comparison for performance (Green). Note the increase in cut-out speed for the hydraulic (DOT) case and subsequent increased power capture at greater wind speeds [26].

Figure 2-2 shows the increased capabilities of hydraulic transmissions at higher wind speeds. While the total efficiency of the hydraulic transmission is less than that of a mechanical one, the heightened level of power capture at greater wind speeds allows the proposed turbine to potentially generate more power. Although this advantage is restricted to higher wind speeds, offshore wind systems generally see faster wind profiles due to reduced surface shear and the taller scale of turbines. This increases the probability that a hydraulic wind turbine will perform better than a mechanical one for offshore applications.

2.3.2 Wind Turbine Components

Offshore wind turbines have become incredibly complex feats of engineering consisting of many different parts. For the purpose of this analysis a set of 18 major components are considered from an NREL design model [71]. Table 1-1 shows a breakdown of each component as it relates the overall turbine. Each component's cost and mass are evaluated for alterations caused by the new transmission.

Table 2-1: A list of major wind turbine components, which was used for cost and mass analysis. The components are shown to inform the reader of parts that may be affected by the gearbox change.

Category	**Component**	
Nacelle	Low Speed Shaft	Bearings
	Gearbox	Mechanical Brake, HS Coupling
	Generator	Variable Speed Electronics
	Yaw Drive & Bearings	Main Frame
	Electrical Connectors	Hydraulic Cooling System
	Nacelle Cover	
Tower	Tower	
Rotor Assembly	Blades	Hub
	Pitch Mechanism	Spin
Sensor Systems	Control,	
	Safety Monitoring,	
	Condition Monitoring	
Grid Connection	Balance of Station[1]	

The top group belongs to the nacelle and contains many of the components affected by the addition of the new transmission. The gearbox is the major component being analyzed in this manuscript and is widely accepted as the highest cost piece to maintain. They are approximately £230,000 (~$350,000) per replacement and one of the most frequent to fail in a study of 2-4 MW offshore turbines [52]. The gearbox will be completely replaced by the new drivetrain and its output shaft will now be located at the base. The generator will be moved to the base along with the variable speed electronics and electrical connectors. The remaining components are not considered to be affected except for the main frame which will be discussed in the methods section. The tower is another major component for the turbine and usually consists of a hollow steel cylindrical column for larger models. Its costs mainly lie in the material required to construct it

[1] Balance of Station describes a set of individual categories containing both hard and soft costs not fully discussed in this paper

which relies on structural load requirements and labor needed for manufacturing. Initial findings on changes to the tower's structural design are covered in the methods section.

The rotor assembly includes: the blades, pitch control, hub and nose cone. The control and condition monitoring system is the internal control system used to optimize the turbine. The rotor assembly is not expected to change, and the condition monitoring system was not fully considered since the reference study for this component is likely outdated in comparison to current control systems in cost. The last system to be analyzed is Balance of Station and it has its own component breakdown with respect to offshore, according to an annual NREL Cost of Wind Energy report [78]. It consists mainly of the support structure, electrical infrastructure and installation of the turbine and makes up on average 52% of installed costs [79]. The breakdown given by these NREL reports shows a difference in allocation for these costs in the overall turbine depending on construction requirements for different offshore projects. A further breakdown of this system is given in another NREL report and our team intends to integrate it into further models [80].

2.4 Methods for Cost Reductions

A flow chart of the methodology used in the study is presented in Figure 2-3. Each block is addressed in the text including where data is found and how calculations were justified.

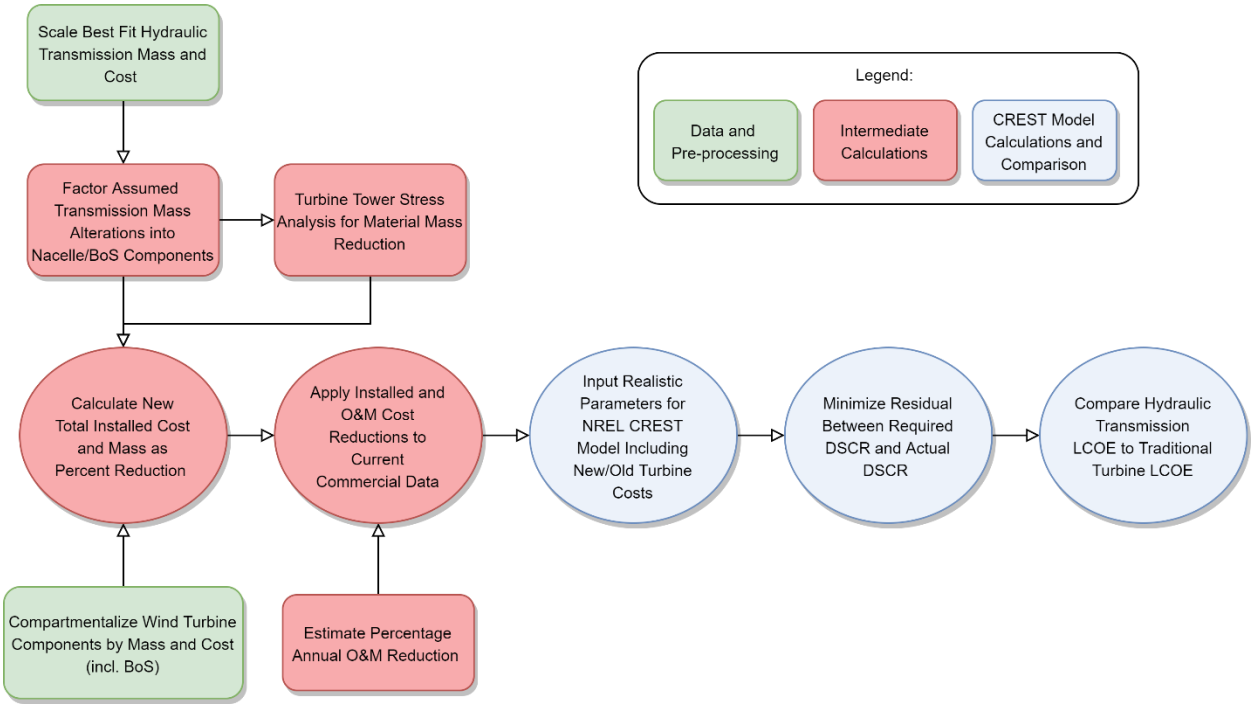

Figure 2-3: A methodology flow chart itemizing the steps taken to standardize turbine component data, apply these reductions to these components, and process the costs into a final comparable levelized cost of electricity.

2.4.1 Transmission and Nacelle Components

An NREL design model of a 3MW shallow depth (10m) offshore wind turbine was analyzed to determine the mass and cost of its various components. A breakdown of how the new hydraulic transmission affects each component, based on the studies [71,78] is given below. The NREL Design and Cost Scaling study is the most thorough description of a wind turbine by parts, covering cost and mass by individual components instead of major categories. The most relevant turbine in the study is a 3 MW design which is used as a framework for this analysis. A larger and more up to date study was produced by NREL but is restricted to internal usage. A set of high, medium and low estimates for cost savings are extracted and derived from IRENA's Cost of Renewable Energy publication [49]. This set of costs encompasses the full range of possible installation costs which are documented from a large pool of newly constructed wind farms around the world.

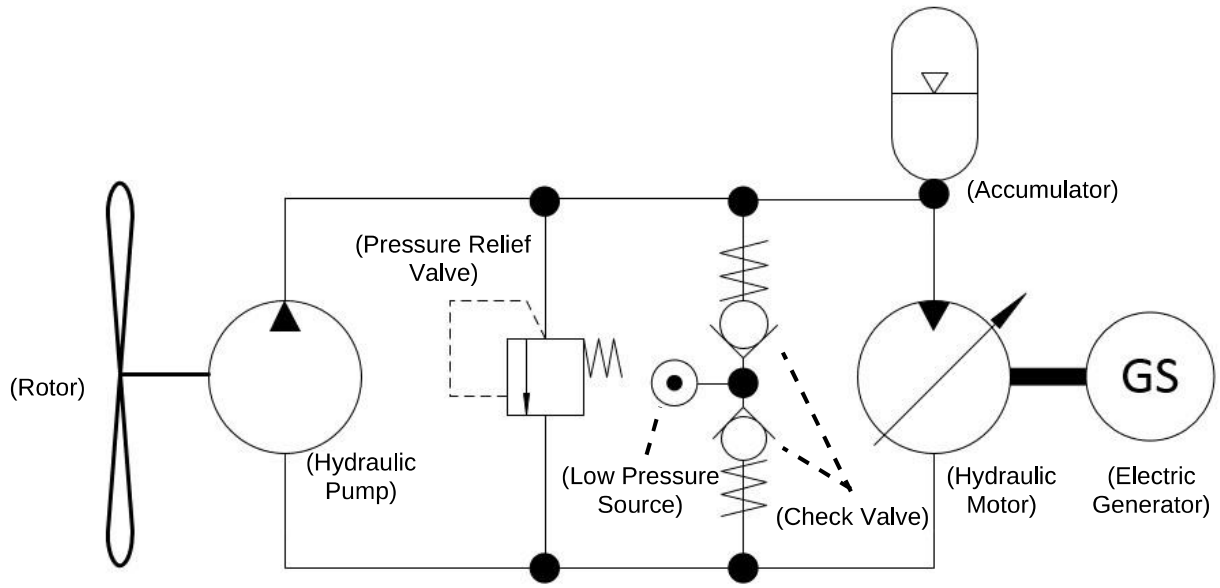

Figure 2-4: A simple ISO schematic of the hydraulic transmission when connected to a wind turbine rotor, which was used in this study. Major moving parts (i.e. pump and motor) are separated by fluid lines which allot for long distance decoupling of the input output shafts. The accumulator shown allows for pressure signal smoothing, providing a stable output RPM.

To start this analysis, a potential real-world version of the hydraulic transmission was designed. A Hagglunds Low Speed High Displacement CBM pump was found to be an adequate commercial fit based on the required displacement and power capacity for the circuit. The quoted price for a 2.2 MW max power unit is about $200,000 [81]. Scaling this pump linearly to fit a 3 MW turbine yields a cost of approximately $272,000. A simple linear relationship is used because pumps of this size are not commercially manufactured, and pricing information is not available without quotes. When adding estimations for the corresponding motor, transmission lines, accumulators, sensors and valves the total cost of the new transmission is valued at $600,000. A simple schematic of the circuit is given in Figure 2-4. This total cost is a liberal estimate and is meant to include any differences in the projected price of the transmission due to sensors and ancillary equipment. The mass of the new pump is 5591 kg when linearly scaled to 3 MW and then rounded up to 6250 kg to include transmission lines, hydraulic peripherals and fluid in the nacelle. This is a 70.2% reduction in transmission mass in the nacelle compared to the mechanical counterpart. The motor, accumulator and total transmission line mass are not considered since they are not relevant for the stress analysis due to the absence of their mass in the nacelle. The mass of

the generator will be located at the base with the output motor of the transmission, as shown in Figure 2-1. This new mass relocation is factored into a stress analysis to determine possible structural design modifications.

Variable Speed Electronics (VSE) are defined in NREL's design models as the system of inverters and converters which make the electrical signals suitable for grid integration and work similarly to a variable frequency drive. Since our system is designed with internal signal smoothing the necessity for these systems will be significantly reduced. We have applied an estimated 0-100% savings to show the difference in cost when signal smoothing is optimized enough to remove the VSE completely.

The main frame is the physical structure that holds the nacelle components in place. Normally, it must be engineered to support high torque/mass components such as the generator and gearbox. The main frame mass is estimated to reduce by 15% from the relocation of the generator and gearbox. Since different manufacturers have different main frame designs, it should not be accurate to simply apply a 1:1 savings with mass reduction, so a lower bound assumption is used. It is worth noting that this is a conservative estimate since the total mass savings in the nacelle is calculated as 35.3% with the movement of the high mass components.

Electrical connectors are defined as including the switchgear and any tower wiring. Since a majority of the components needing electrical connections are now housed at the base, the necessity for long wiring will be reduced. We estimate 20-70% cost savings for these components based on the underlying materials shown in the NREL design model [71]. The remaining nacelle components are not altered in any way.

2.4.2 Tower Considerations

While a significant reduction of mass in the nacelle takes place, this should not affect the structural design of the tower, which is constrained by the bending moment generated at the base of the tower due to the drag force experienced by the rotor, not the internal compression forces. The stresses generated by this drag force are many times larger than those produced by the mass in the nacelle. Table 2-2 presents an estimate of the stresses calculated using simple compression on bending stresses using a reference 5 MW turbine model [82]. This turbine is used because it has the most comprehensive and up-to-date dimensioning parameters that could be found.

Maximum bending stresses on an 87.60-m tall tower with top and bottom thickness of 20 mm and 27 mm and top and bottom diameters of 3.87 m and 6 m respectively, are calculated using the provided thrust force, reported as 600,000 N at 10 m/s. The starting nacelle mass is given as 240,000 kg, with additional hub mass of 56,780 kg and individual blade mass of 17,740 kg. The maximum bending stress equation is used with a moment of inertia of a ring with inner and outer diameters. The drag force of the wind along the length of the tower is neglected. The entire height of the tower is considered but the additional height of the nacelle is not. The output stresses are as follows:

Table 2-2: A list of major wind turbine components, which was used for cost and mass analysis. The components are shown to inform the reader of parts that may be affected by the gearbox change.

Stress Component	**Stress (kPa)**
Tower Top	1.419×10^7
Tower Middle	1.332×10^7
Tower Bottom	1.350×10^7
Rotation Around the Base	6.979×10^7

As one can see from the output of Table 2-2, the stresses produced by the thrust from the rotor are much larger than the compressive stresses at the three points along the tower. While they are the same order of magnitude, further analysis is required to justify any changes in tower thickness. The reader is encouraged to look at a study which evaluated how a hydraulic transmission would change tower thickness [28]. In this analysis, the researchers found that utilizing a hydraulic transmission, in the same configuration as stated above, will reduce tower mass by as much as 33-50% through thickness changes. The savings was found by calculating the reduction to top mass then systematically altering tower thickness or diameter until the natural frequency safety factor of the original design was achieved. This significantly decreases the capital cost of the wind turbine tower and should be considered as one of the potential benefits of the new transmission.

2.4.3 Balance of Station Components

A breakdown for Balance of Station on a component wide basis is taken from the NREL 2015 Cost of Wind Energy publication [78]. Balance of Station is given as a 52% contribution to the overall installed cost of an offshore wind turbine in this study. In order to stay consistent with the older design model, each component part is taken as its individual contribution to balance of station, not the installed cost as a whole. Assembly, transport and installation costs are systematically reduced by 10-30% as a result of reduced crane usage and ease of nacelle erection. Furthermore, electrical infrastructure may be reduced by as much as 75% of its original value to account for a variety of new cost optimizations such as new configurations for generators and grid connection, which are possible with a hydraulic transmission [83]. Most notably the combined Pelton Turbine configuration shown in Delft University's DOT [26], which consolidates the power production of multiple turbines into one generator, greatly reduces wiring to the farm sub-station and generator costs. The support structure is reduced by 22 -30%, the lower end being the total top mass relocated to the base and the higher end adding increased benefits not immediately apparent. These savings add to a total range of reductions of 16 - 36% over the original balance of station costs.

2.4.4 Cost of Renewable Energy Spreadsheet Tool Parameters

Factoring all of these savings into the design model profile yields a total cost savings range of 5.36-24.0% over initial installed costs. This range will be applied to the IRENA installed cost estimates of $1958/kW-$5062/kW [49]. A simple average between those two values is also taken as well as the average between the cost savings range. Table 2-3 shows the list of remaining parameters which are changed in the NREL Cost of Renewable Energy Spreadsheet Tool (CREST) model used to compute Levelized Cost of Electricity (LCOE) [84]. Each of these parameters are set based on either supporting references or given methodology.

Table 2-3: Input parameters changed in the CREST model spreadsheet created by NREL for the cost estimates of a traditional turbine. Installed costs and O&M are reduced by 5.36-24.0% and 0-10% respectively for the hydraulic turbine comparison.

Category	Sub-Category	Value
Capital Costs		
	Installed Cost	1958-5062 ($/kW)[49]
Operation & Maintenance		
	Fixed Operation & Maintenance	127 ($/kWh)[19,79,85–89]
Project Size and Performance		
	Nameplate Capacity	3 (MW)
	Net Capacity Factor	42 (%)[90]
	Project Useful Life	25 (years)[91]
Permanent Financing		
	Debt Term	25 (years)
	Interest Rate	4.4 (%)[16,89,92]
	Debt Service Coverage Ratio (DSCR)	1.3
Forecasted Market Value of Production		
	Value of Energy	0.12 ($/kWh)[93,94]
	Market Value Escalation Rate	3 (%)[16,93,94]

After the chosen parameters are set in the model, the Actual Minimum Annual DSCR is minimized against the required DSCR by incrementally raising or lowering the percentage of hard debt financed. Annual DSCR is a measure of the annual net operating cash flow that is available to pay annual debt obligations and is assumed to be 1.3. This value is slightly increased from the model predefined 1.2 to reflect a healthy project with annual net operating income 30% larger than debt obligations. Installed costs are set to 9 separate values consistent with low, medium and high

costs from IRENA discussed above as well as each value adjusted for the high, medium and low savings values. Finally, these are run twice with fixed and variable costs of $127/kW/yr and $0.025/kWh both reduced by 0% and 10%. The resulting LCOE estimates are then adjusted from ¢/kWh to $/MWh.

2.5 Cost Calculations

2.5.1 Installed Cost Reductions

Installed costs comprise half of the overall cost equation of setting up a turbine or full wind farm, the other part being operation and maintenance. Installed costs include the material cost, manufacturing and installation setup for the project at hand. For the purpose of this study the breakdown for material cost for the turbine will be derived from the NREL design scaling model, whose underlying work first considered American/European markets [71]. The balance of station average estimates for offshore wind were referenced above and taken from a combination of NREL's design models and Cost of Wind Energy reviews [71,78]. Together these costs are individually assessed and summed to calculate the total expected savings for installation costs.

Table 2-4 shows the mass contributions of three components in the nacelle which are affected by the alteration. As displayed, the mass of the three parts: (i) Gearbox, (ii) Generator and (iii) Main Frame are reduced individually and contribute to a total nacelle mass reduction of 35.3%.

Table 2-4: Mass estimations for a 3 MW wind turbine, its new mass in the nacelle with the hydraulic drivetrain and the savings due to the conversion to a hydraulic transmission [71]. Notice the major reduction to the gearbox component, now replaced by the pump, as well as the entire removal of the generator. The main frame is also scaled to reflect the reduced need to anchor massive components.

Component	Original Mass [kg]	New Mass [kg]	Savings [%]
Gearbox	20,973	6,250[2]	70.2
Electric Generator	10,426	0	100
Main frame	40,426	34,362	15

[2] This mass is associated only with the new hydraulic transmission and does not imply any residual mass from the mechanical gearbox.

Table 2-5 shows the estimated cost savings range for four turbine components: (i) Gearbox, (ii) Variable Speed Electronics, (iii) Main Frame and (iv) Electrical Connectors. The cost estimates for the gearbox were scaled from the Hagglunds pump using an assumed simple linear relationship between rated power and cost. Variable Speed Electronics (VSE) control electrical grid compatibility. American grid systems have permitted fluctuations of ±0.5Hz from the standard 60Hz frequency. Outside of this range, load shedding and other methods must be used to ensure that the grid does not destabilize [95,96]. If the control system for the transmission is optimized to keep output signals within this band then the VSE are not needed. The savings allocated to the Main Frame is taken directly from the reduction in nacelle mass. This value is expected to correlate very highly with the mass of high torque components in the nacelle which must be anchored properly. NREL's Design Model shows a power relationship between rotor diameter and Mainframe cost and mass yet changes coefficients for different gearbox configurations [71]. Rotor diameter does not necessarily correlate with nacelle mass in commercial turbines due to cost optimization so the relationship between mainframe mass and nacelle mass is treated as an assumption.

Table 2-5: Cost of nacelle components being altered and a high and low estimate for reductions [78]. The gearbox and mainframe components have a constant change regardless due to assumed complete removal of the generator and mechanical gearbox. Variable speed electronics may or may not be removed depending on the hydraulic transmission output frequency. Electrical connectors are considered to change based on relocation of electrical components such as the generator.

Component	**Old Cost [$1000's]**	**New Cost High, Percent Change [$1000's], [%]**	**New Cost Low, Percent Change [$1000's], [%]**
Gearbox	408	$600, 147%	$600, 147%
Variable Speed Electronics	266	$266, 0%	$0, 100%
Main Frame	168	$108.8, 35.3%	$108.8, 35.3%
Electric Connections	150	$120, 80%	$45, 30%

Balance of Station is handled separately; Table 2-6 shows the estimates in savings for three components that are expected to be affected by the new design: (i) Assembly and Installation, (ii) Electrical Infrastructure and (iii) Support Structure. Assembly and Installation may decrease by as much as 10-30% as a result of predictions regarding the enhanced ease of erecting offshore turbines and reducing crane costs. Electrical Infrastructure is a complex component and an assumed range of 0-75% savings is applied to it. If one considers the Pelton turbine configuration in the Delft University study [26], this infrastructure can be greatly reduced, hence the higher end estimate. If a single generator per turbine design is used, then the savings is expected to be minimal [35]. The Support Structure is an extremely complicated foundation that enables offshore turbines to exist in harsh environments. There are several designs currently in use and our team expects that the greatest savings will be applied to the floating spar buoy/semi-submersible configuration due to buoyancy forces and mass redistribution [97–99]. By relocating the center of mass on the turbine the buoyancy properties required by the sub-structure can be reduced. The 22.3% low end savings is derived from the redistribution of top-mass to the base.

Table 2-6: Balance of System (BoS) components for the wind turbine and their respective contribution to overall cost of BoS. High and low cost contribution estimates for new transmission, reduced from the first column [3].

Component	**Old Percentage [%]**	**New Percentage Low [%]**	**New Percentage High [%]**
Assembly, transport & installation	38.5	26.9	34.6
Electrical Infrastructure	19.2	4.8	19.2
Support structure	34.6	24.2	26.7

The sum total of these estimated costs savings results in a relatively wide range of installed cost reductions. Given the low and high estimates in the tables provided, our team estimates a range of 5.36-24.0% savings on the overall installed cost of the turbine and its infrastructure. Figure 2-5 below shows a graphical representation of the reduction to each component over the 3 MW reference turbine created by NREL [71]. Marinization is added to the category list as an immutable

cost for all offshore wind turbines. Each component discussed above belongs to ones of the categories shown below.

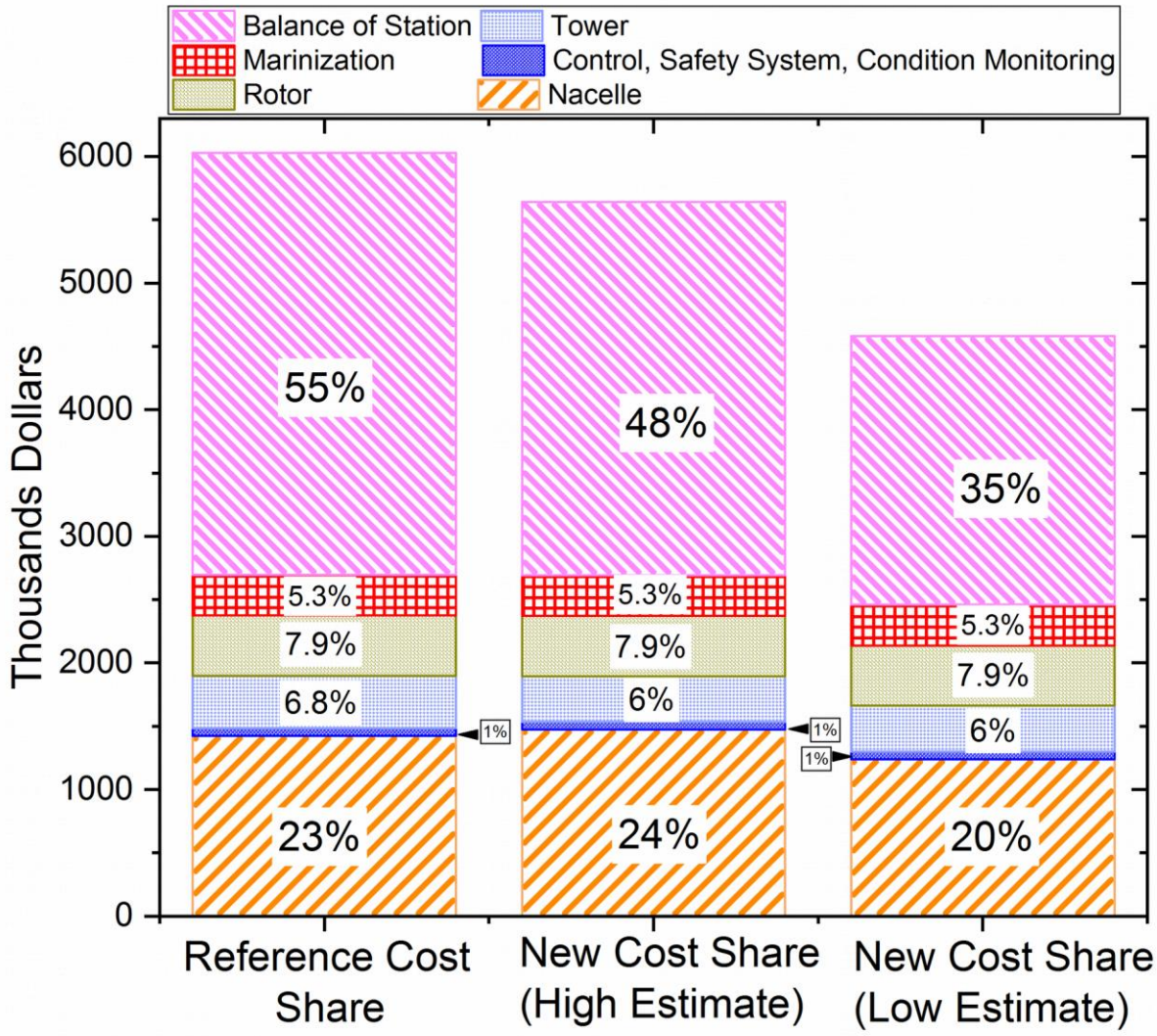

Figure 2-5: A comprehensive cost breakdown of the wind turbines variants, with 2011 data: Left column: A reference mechanical transmission wind turbine is broken down into its relative installed cost components [71]. Middle column: High cost low savings (5.36%) estimates result from alterations to these major categories. Right column: Low cost high savings (24.0%) estimates are also shown.

In Figure 2-5, the columns are split into 6 major categories which make up the costs associated with offshore wind turbines. Based on the mass and cost reductions discussed above, many of these categories shrink with respect to the final cost of the entire turbine. It is important to note that the physical dollar value of the reference turbine is not used since it was derived in 2011[71] and more current installed cost data exists.

As to be expected, the balance of station and nacelle categories see the most reduction in cost. The middle column may seem counterintuitive since it shows a larger contribution for the nacelle. This is caused by the assumption that the variable speed electronics are not replaced for the high cost estimate, which contribute to a large portion of nacelle cost. Balance of station is clearly the most sensitive to the utilization of a hydraulic transmission. Many of its underlying components are altered by the new transmission, and in potentially more cost significant ways.

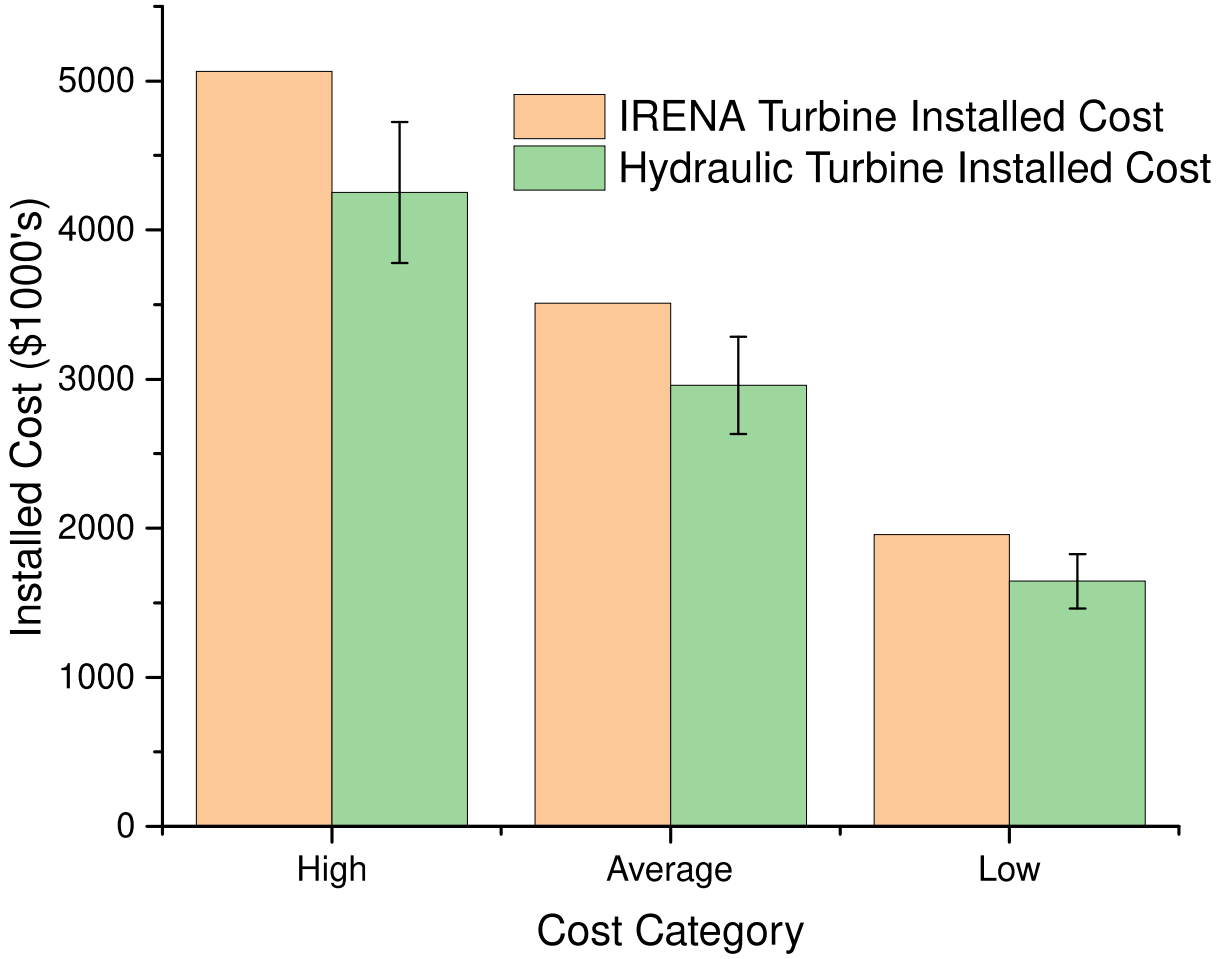

Figure 2-6: Expected savings for turbines of different costs (High, Average, Low). Standard turbine data from IRENA (2017) (orange) [1]. These ranges reflect a variety of projects from around the world, each with unique design requirements. The ranges for savings due to the hydraulic transmission are applied to the IRENA values to produce the final installed costs (green).

Figure 2-6 shows a breakdown of the actual installed costs used for the LCOE analysis. The percent changes calculated from the design analysis above are applied to these present-day

costs. In terms of raw dollar amount, high cost turbines clearly benefit the most from utilizing a hydraulic transmission.

2.5.2 Operation and Maintenance

Operation and Maintenance costs are difficult to estimate in a potential wind turbine project. Not only does it encompass the scheduled upkeep of the turbine and replacement of parts, but it takes into account the relative cost of paying workers in different regions and relies on distance from shore/port, available workforce and size of the project [79,80,86].

The program used for our analysis requires O&M to be broken into two categories, fixed and variable costs. As the name suggests, fixed costs are associated with scheduled maintenance such as inspections and predetermined replacements. Variable costs are associated with random or unforeseen costs such as emergency repairs. Several categories make up each of these costs [19,85–89]. Since it is currently difficult to determine the overall reduction in fixed costs, our team is assessing how the relocation of the components to the base would affect scheduled and unscheduled maintenance. The new transmission is expected to have a longer lifespan than traditional gearboxes and will be easier and less costly to repair at the base of the turbine [100,101]. We estimated that O&M may be reduced by up to 10%, shared amongst unscheduled and scheduled maintenance on all components relocated or altered by the replacement of the transmission.

2.6 Levelized Cost of Electricity

Levelized Cost of Electricity (LCOE) is a commonly used metric to compare the economic viability of different power systems. It is defined as [31],

$$LCOE = \frac{\sum_{t=1}^{n} \frac{I_t + M_t + F_t}{(1+r)^t}}{\sum_{t=1}^{n} \frac{E_t}{(1+r)^t}}, \qquad (2\text{-}1)$$

where I_t = Investment expenditures in year t, M_t = Operations and maintenance expenditures in year t, F_t = Fuel expenditures in year t (if applicable), E_t = Electricity generation in year t, r = Current market discount rate, and n = Economic life of the system. The LCOE represents the sum

total discounted expenditures for construction, maintenance and fuel over the life of the system divided by the estimated production of energy over the system's lifespan. By standardizing costs by energy production, projects of any fuel source, life span and capacity can be compared for commercial application.

CREST, an advanced analysis spreadsheet developed by NREL, is used to calculate this metric. The spreadsheet is extremely comprehensive and is generally used for policy making and broad range strategic investments. There are several altered metrics that our team estimated for an arbitrary offshore wind project. The range of $1958/kW - $5062/kW as well as the simple average between them are used as initial inputs for installed costs, extracted from IRENA publications [49]. Average fixed operation and maintenance costs were reported as $127/kW/yr [89] and since no better estimate was found, the default value of $0.025/kWh is used for variable O&M.

2.7 Data Resolution and Sensitivity Considerations

The precision of the data used in the analysis is restricted to how frequently major studies record costs on wind turbine components and complete projects. The core of the analysis is based on an NREL study breaking down the installed component costs of a turbine into basic categories [71]. The age of the study makes the numbers reported outdated and new versions of the study are not publicly available. Therefore, the percent contribution of component costs and masses are used to calculate the final installed cost and mass reduction due to the application of a hydraulic transmission. The installed cost ranges used in the LCOE model are tracked and reported annually by IRENA [49]. The CREST model produced by NREL takes the economic inputs, calculated or found in the above methodology, and returns the first year LCOE. Real-world meteorological data is not considered in the model but rather the input capacity factor is multiplied by the number of hours in a year (8760) and the nameplate generator capacity to retrieve the annualized energy production [84]. While it may not perfectly reflect a particular wind project, this approach makes the results more generalized.

The assumptions used in calculating the installed cost reductions are chosen in a way to encompass the widest range of possible real-world results. This was designed to act like an internal confidence interval for the reductions to installed cost. Because the underlying assumptions are not entirely justifiable, a wide range of values accounts for the best- and worst-case scenarios. Additionally, ranges for current installed costs are considered as secondary confidence intervals

as a way to fully describe the spectrum of commercial wind projects worldwide. The sensitivity of the financing is considered outside the scope of this study and therefore not fully evaluated on its own. The effects of changes in financing is briefly mentioned in the discussion section.

2.8 Results and Discussion

Figure 2-7 shows the full range of savings over different cost turbines and alterations to O&M. The baseline LCOE, (as calculated with the reference installed/O&M costs), for high, average and low installed cost turbines are $155.5/MWh, $127.5/MWh and $97.50/MWh respectively [49]. This gives three intervals of possible savings. The savings on low cost turbines shows a possible range of 1.03-16.4% while the high cost turbines save anywhere from 3.86-19.3% over their original price. However, we are more confident with the average savings for medium cost turbines of 3.92-18.8% due to the assumptions in the underlying cost reductions. It is worth noting, that an "average" cost savings translates to tens of millions of dollars for a large offshore farm over the course of its lifespan (e.g., 20-25 years).

The savings come from a culmination of several changes that can be made if the turbine is redesigned around the transmission. With less mass to secure, the mainframe material can be reduced, variable speed electronics can be entirely removed and the support structure for the balance of station component can be optimized with the change to the turbine's center of mass. Additional changes to the wiring and other construction considerations amount to the full savings seen in the installed cost of the turbine. The blanket percent reduction applied to operation and maintenance was due to an assumption made about the underlying components which were not covered in depth in this study. By viewing the above LCOE equation and factoring in the changes to installed cost and operation and maintenance, one can see the how each part contributed to the overall reduction. Terms for loans on the project can be added to the numerator as additional cost terms but changes in the cash flows of the project from altering these values are beyond the scope of this study.

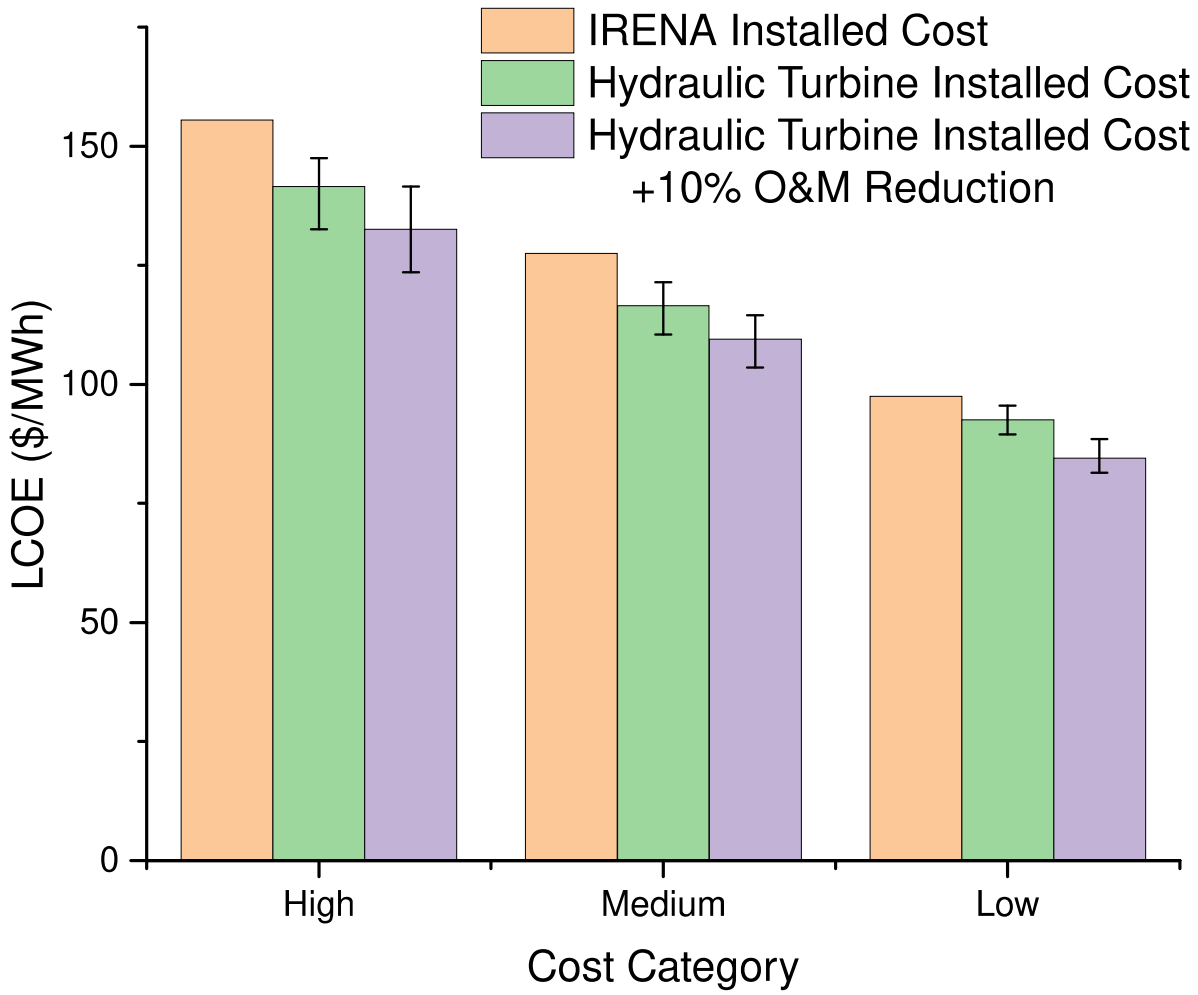

Figure 2-7: Shown: the range of LCOE savings for high, average and low cost turbines. Reference traditional turbine values from IRENA (orange) [49]. High, medium and low cost reduction estimates are applied to the IRENA installed costs (green). An additional high, medium and low estimate is given to include a 10% reduction to O&M as well as the installed cost reduction (purple). Each estimate has a corresponding range of savings based on different distributions of allocated costs.

Although these results rely on ranges for component cost reduction, there are many limiting factors that were present in the research leading up to the CREST calculations that require discussion. Reductions to electrical connections, electrical infrastructure and assembly, transport and installation were unable to be substantiated with research data, yet they clearly may be affected by the replacement of the transmission. The ranges given to these factors should be treated as assumptions. Ranges estimated for support structure and main frame are also unable to be directly substantiated without considerable design work on existing parts which are not readily available,

and therefore should be considered assumptions as well. The 10% range given to operation and maintenance was estimated from a variety of sources but there does not exist a quantitative model for how mass changes affect these costs, therefore this range is also considered an assumption. Even though the estimates present in this study are unable to be directly validated with existing research, the purpose of this analysis is to identify potential economic benefits of using a hydraulic transmission in a wind turbine at a component level and attempt to quantify the dollar value given these assumed changes.

The results of the study show a significant decrease in the cost of an offshore wind turbine if a hydraulic transmission is used instead of a mechanical one. Very few studies granularly analyze the contribution that mass and technology changes have on the structure of wind turbines for manufacturing and construction. Most chose to analyze the productivity of a wind turbine caused by a change in efficiency from technological/operational innovation rather than through material costs. As such, there have been no conflicting studies that would lead the authors to believe that these findings are invalid except for the tower portion of the study, where the group was unable to corroborate an existing study and justify its extensive savings from thickness reduction [28]. The analysis presented in this manuscript falls short of evaluating the resonance design parameter which is why the mass reduction was not uncovered. The authors encourage readers to continue to the work discussed here and further justify component contributions such as to the support structure and main frame of the wind turbines. Additionally, the dynamics of the floating sub-systems can provide a wealth of new research when considering changes in mass to the above-water turbine itself.

An important part of this analysis for further consideration would be the permanent financing portion of the CREST model. Through use of the model with various input parameters, it was learned that the sensitivity of the final LCOE generated is heavily reliant on the interest rate for hard debt costs. Tax brackets, DSCR and other costs in the financing section were not addressed in this analysis, like above however, the final LCOE becomes highly sensitive to changes in these underlying values, therefore, while important to reduce installed and maintenance costs, at this stage in the industry, better financing solutions may provide a larger benefit to project developers.

2.9 Conclusion

The analysis conducted above evaluates how the levelized cost of offshore wind energy changes through the replacement of a mechanical transmission with a hydraulic transmission. Although the hydraulic transmission can be used in land-based turbines, our study focuses on its benefits for offshore applications. The cost and mass associated with each turbine component is shown, including how much these parameters may change under the replacement. Careful analysis concluded that about 35.3% of the nacelle mass can be relocated to be tower base and an average installed cost savings of 5.36-24.0% can occur from turbine redesigning around the new transmission. The physical system cost is then combined with annual operation and maintenance using the CREST spreadsheet and conservative financing is applied to the test project. The results shown in the study, i.e. relocating of nacelle mass, convenient positioning of regularly maintained components to the base and obsolescence of now redundant technology predicate an average savings of 3.92-18.8% on the LCOE that wind turbine producers and operators will see if there is full adoption of the new hydraulic transmission.

This study should be considered as a framework for potential future savings for the offshore wind turbine industry as a whole. Not all of the benefits shown are immediate and will require a joint effort from the manufacturers of different turbine components (specifically for multi-megawatt pumps) to be fully exploited. Additionally, the underlying data provided by IRENA as well as the wide variation in cost associated with real world wind farms forces a wide range of savings to be calculated instead of a precise one. As we move forward, our team will focus on optimizing the transmission for large scale turbines and conduct a more thorough design analyses for the tower and balance of station components. As advances are made in hydraulic components, production costs will likely decline, this is particularly true for pumps making the system even more attractive. Even as an initial assessment, the numbers reported in this study indicate there is actionable cost savings to be realized with the usage of a hydraulic transmission.

3. COMBATTING WATER SCARCITY AND SOCIO-ECONOMIC DISTRESS ALONG THE US-MEXICO BORDER USING RENEWABLE POWERED DESALINATION

3.1 Abstract

Access to sustainable clean water is a necessity for any successful civilization. The US-Mexico border has been experiencing a decline in the availability of this critical resource, stemming from mismanagement and exacerbated by climate change. If water is not adequately overseen, the region will be unable to support local societies and industry, effecting millions of inhabitants. A vision, articulated in Scientific American in 2019, showed the potential for the development of a technology innovation park along the border which would provide sustainable water using renewable powered desalination. A version of this concept is demonstrated with configurations of coastal Seawater Reverse Osmosis desalination plants, sized to meet the public water demand of ~1000 MGal/day (~3.79 Mm3/day). The desalination and distribution of clean water is powered by offshore wind and onshore solar PV farms, which transfer energy over High Voltage Direct Current cables. One-hundred eight renewable variations were simulated and demonstrated the ability to supply clean water at a levelized cost of 2.00-3.52 $/m3. When compared to 27 fossil fuel configurations, renewable powered variations avert adding the equivalent of 1.8-2,100,000 cars worth of CO2 pollution per year, avoid withdrawing the equivalent of 65-75,000 US households worth of water for power generation annually and add potentially over 100,000 more jobs. As water scarcity along the border becomes more prevalent, alternative sources of sustainable water will be crucial for bringing long term resource stability to the region.

3.2 Graphical Abstract

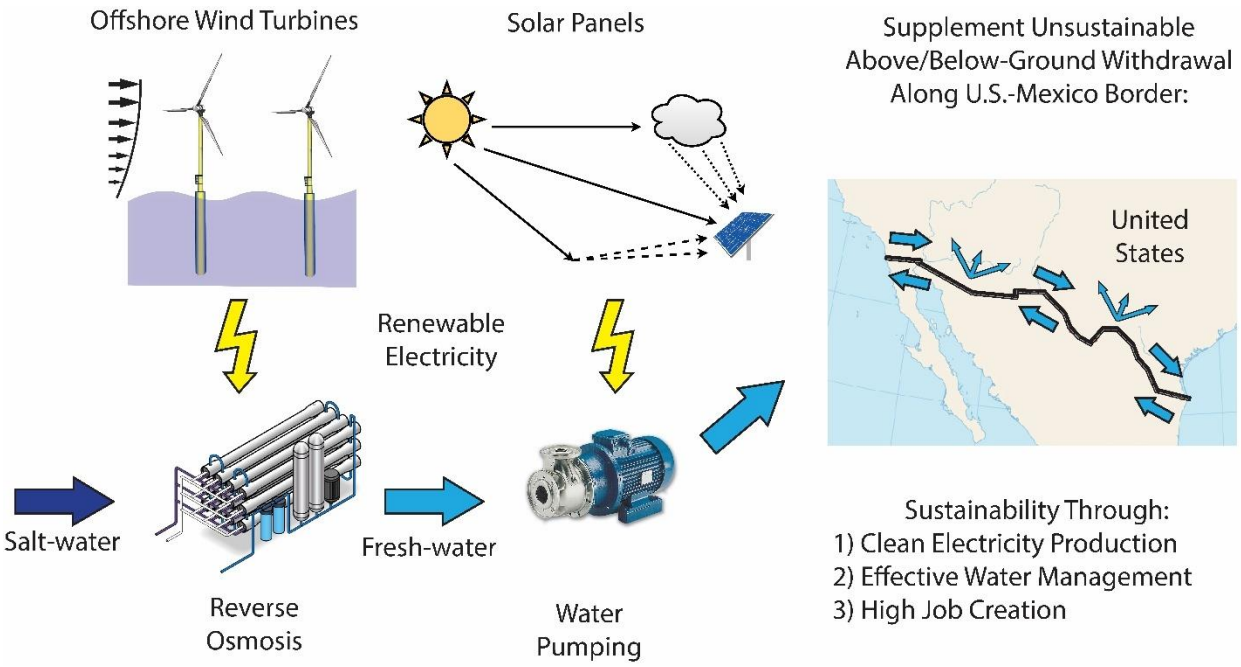

3.3 Introduction

In 2019, a large consortium of scientists and engineers led by Purdue University laid out a vision for supplying energy and water along the US-Mexico border to develop a corridor for technological innovation and agriculture [102–104]. The theory proposed using desalination and renewable energy to create a zero-emission source of sustainable water. In this article we provide an in-depth techno-economic analysis of such a concept with an emphasis on water sustainability in the region.

Mexico is a top trading partner with the US in terms of goods and services[105], yet the border between these two countries is a contentious region where crime, poverty and resource scarcity are prevalent and agreements between the two countries to share natural resources have been largely unsuccessful[46,47,106]. Aquifers and large rivers historically satisfied the agricultural and basic needs of the area; however, the natural replenishment cycle has become increasingly inadequate to sustain the growing regional demands [44,107,108]. Sources such as the Rio Grande River basin and Colorado River are already experiencing detrimental shortages[106], hindering groundwater recharge. US counties along the border draw approximately 47%[109] of their supply from these now non-renewable aquifers so local populations must significantly reduce water usage and/or

import expensive water from neighboring communities. Otherwise, recharge cycles will cease to operate effectively, making agricultural and societal expansion all but impossible.

With the price of water across the US escalating[110], creating, rather than importing alternative sources of freshwater will likely be necessary. Seawater desalination is the logical option for providing a sustainable auxiliary supply. In contrast, on-site water reuse is limited by both the recovery ratios of the purification process and by what can be returned to local distribution networks. Brackish water desalination is not ideal either as it would draw from the same strained aquifers and rivers.

The two main saltwater desalination types, thermal and membrane based, were historically competitive at large scale, but membrane based Reverse Osmosis (RO) is often the most energy and cost effective[111–117]. Many regions around the world, such as the Middle East, India and South Africa, have embraced using saltwater RO for water security [38,40,118–120]. The US-Mexico border mostly spans landlocked North American territory. This means the only accessible seawater feed sources are at the Pacific and Gulf coasts, necessitating a dedicated infrastructure to deliver the water.

Fortunately, the renewable offshore wind[121–125] and solar[125–129] resources around the border provide satisfactory energy for desalination and distribution respectively. Advancements in these renewable technologies have driven down prices enough to be cost competitive with fossil fuel[130]. Hydraulic drivetrains in wind turbines[22,26–30] and tracking systems for solar panels[20,21,23–25] are a few examples of improvements which can bring down the cost of energy for integrated infrastructure projects such as this one.

The proposed RO plant(s) are the largest ever designed[131] with a capacity of 1000 MGal/day (3.79 Mm^3/day), and were simulated using three different process efficiencies[112]. A 30m resolution geospatial terrain and elevation map of the entire border was constructed[132] and used to calculate inland pumping energy intensity. Gulf and Pacific offshore wind farms were located in areas of high average wind speed and sized by modeling Weibull profiles and matching annual energy production with desalination energy consumption[133–136]. To satisfy the almost 2 GW needed for distribution, five potential solar farms along the pipeline were modeled using optimized tilted and one-axis tracking panels[137,138]. Solar farms were chosen over onshore wind because they provide better techno-economic performance along the full length of the border.

One-hundred eight renewable variations, and another 27 using fossil fuel and existing grid energy, were simulated to demonstrate a range of real-world costs and potential configurations. Results showed that renewable-driven variations were cost competitive with "environmentally friendly" fossil fuels. More importantly, renewable variations significantly outperformed fossil fuels in life-time operational water withdrawal, life-time CO2 emissions and systemic job creation[139]. The objective of the project is to design a sustainable clean water infrastructure that is not only beneficial to the population but environmentally responsible. The economic and environmental competitiveness of renewables to power the project allows for the facilitation of both. In doing so, the US-Mexico border can evolve from a resource strained region into one of economic prosperity.

3.4 US-Mexico Transboundary Surface and Groundwater Assessment

While the purpose of this project is to design a sustainable clean water infrastructure for the American side of the US-Mexico border, also of great interest are the underlying socio-political issues that plague the area. As previously stated, the US and Mexican government have attempted to share the natural water resources along the border. Resources such as the Rio Grande river basin and San Pedro aquifer straddle the border and thus both parties are entitled to their benefits. To handle these finite sources of water, the U.S. and Mexico entered into International Transboundary Agreements covering above and below ground resources[44–47]. The Mexican Water Treaty of 1994 has been used as a policy framework for water use and disbursement along the border.

As industry and society have expanded on both sides of the border the need for water has grown drastically. Coupling this with unprecedented droughts and dried riverbeds on the Mexican side has left the region fighting over increasingly scarce resources [46,47,106,140]. Now a commonplace occurrence, Mexican farmers have been left with a deficiency of irrigation water as agreed-upon amounts are exported to the United States, harming the socio-economic evolution of the northern region.

At the time of writing, Mexican farmers took up arms and occupied a major dam in Chihuahua which funnels water into Mexico or back into America [48]. America argues that Mexico has not provided their agreed upon water exports to the US and has requested they be fulfilled. Due to environmental and socio-economic factors plaguing Mexico, they will be unable to provide this water without leaving native residents with a crippling irrigation deficit. Mexico may make good

on its promise by redistributing aquifer drinking water from other regions which could leave the country open to widespread water shortages if droughts continue.

Clearly there is a major sustainability issue around the shared water resources in the region and without thorough policy changes**,** this problem will only worsen. However, it is important to understand that the regional resources are finite, and no amount of delegation will solve water shortages as local communities grow. Societies in the region will spiral into disarray as the most basic resource for life, agriculture and industry dries up. Alternative sources of water, such as the framework proposed here, are crucial for long-term growth and prosperity. While the proposed project currently only accounts for a US based infrastructure for water delivery, by offsetting portions of American usage, more of the natural resources can be shared with Mexico.

The project hopes to eventually provide socio-economic stimulation to both sides of the border region through reallocation of these resources, creating a future zone of commercial and economic prosperity. Modular expansions can be made to the infrastructure to promote a new sustainable transboundary resource network where both parties can responsibly satisfy their regional needs.

3.5 Water Profile and Reservoir Design

3.5.1 Water Requirements

As with most large-scale resource infrastructure projects, determining the quantity of the target resource to offset or supplement can be a difficult and subjective task. The water requirements along the US-Mexico border include cities and towns on or near the border that contribute to the total water withdrawals in the region. To characterize this, United States Geological Survey (USGS) water data was compiled for the entire set of U.S. counties which border with Mexico[109]. These counties were selected due to their proximity to the border and practical amount of water to be offset for a 1st iteration design. These boundaries may change with future iterations.

Although irrigation represents the largest source of water withdrawal (~79% of total withdrawals and ~74% of total consumption), the project cannot compete with these often extremely inexpensive and privately obtained resources[141–143]. Additionally, commercial/industrial data were too incomplete to confidently model price competition and total withdrawals. Instead, the project was designed to supplement the public supply of water provided

by local municipalities. This sector has both a substantial enough size (~17% of withdrawals and ~22% of consumption) to offset a large portion of water use and facilitates engagement in a much more cost-competitive market. While the public supply withdrawal, equal to consumption, in the region is approximately 973 MGal/day (3.68 Mm^3/day) and sustains over 7.5 million people, the project is oversized slightly to account for 1000 MGal/day (~3.79 Mm^3/day) of capacity for ease of planning. Figure 3-1 shows the total breakdown of water withdrawal in counties along the border.

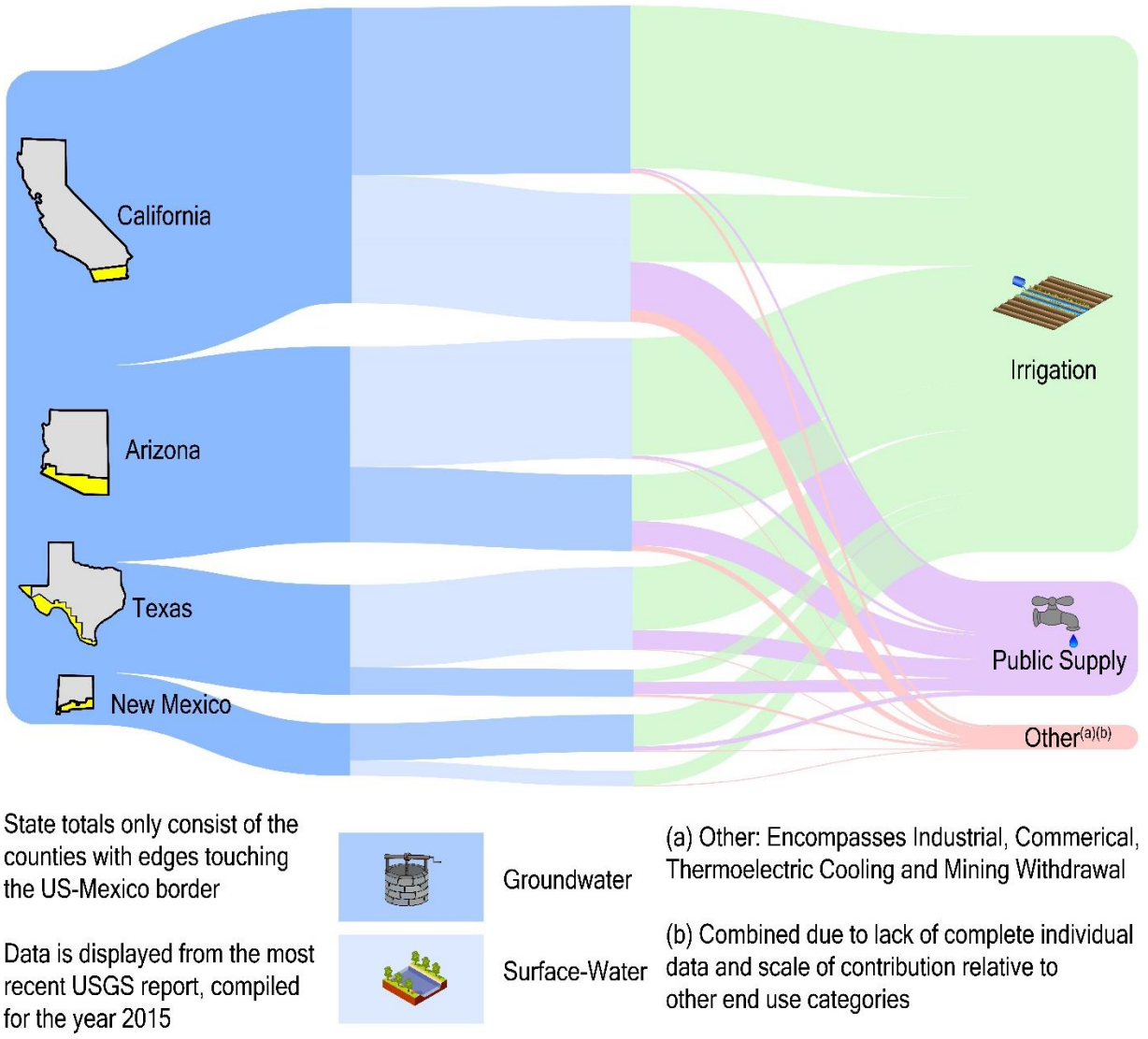

Figure 3-1: Breakdown of the total water withdrawal in counties bordering Mexico (highlighted in yellow), separated by state, groundwater (47%) vs. surface-water (53%) and end-use sector. Public supply is provided by local municipalities but the remaining end-use sectors obtain water by private means[109]. The other category consists of commercial, industrial, power plant, aquaculture and private domestic withdrawal. Percent contributions of Irrigation, Public Supply and Other to withdrawal and consumption are approximately 79%, 17%, 4% and 74%, 22%, 4% respectively.

3.5.2 Reservoir Sizing and Future Hydro-Electric Storage Considerations

The extensive pumping network may benefit from a reservoir to help stabilize the distribution portion of the project and provide long term water storage for drought protection. Consequently, a reservoir was incorporated mid-way along the pumping infrastructure. The reservoir is sized to store 180 days of public water for the region which equates to about 681 Mm^3, plus an additional 5% dead volume for design purposes[144]. Reservoirs not only provide water storage but also have the future potential to be used as distributed hydroelectric batteries given the right environment. Hydroelectric storage is one of the most cost-effective forms of long-duration energy storage and combining it with this project could improve the lifetime economics[145]. Ambitiously, it may even stand as a buffer for national renewable energy integration, which is plagued by the necessity for large scale storage[130,146–148].

The topographic profile along the border indicates several regions of substantial elevation change compatible with Modular-Pumped Storage Hydro (m-PSH)[146]. The closed loop variation of this technology cycles water between isolated low and high elevation reservoirs and is comparable to a large rechargeable battery. Since water storage is already of importance to the project infrastructure, it may be advantageous to integrate this modular technology along the pipeline for the additional energy benefits.

3.6 Border Topography, Pumping Load and Pipeline Characterization

To accurately calculate the energy requirements of the pumping infrastructure, 30m resolution topographical map of the US-Mexico border was created using several Digital Elevation Models (DEMs) from the United States Geological Survey Shuttle Reconnaissance Topography Mission (USGS SRTM) 1-arc second database[132]. Figure 3-2 shows this model and the extracted elevation profile from coast to coast along the border. Topographic and parameter maps are presented in Figures 3-2,3 as a visual representation of pumping requirements and locations of major infrastructure sites. Please note that the exact route taken by the pipeline is likely to change. Preliminary models do not account for circumventing wildlife preserves, state/national parks or other restricted areas. The route presented here is intended only for demonstrating approximate pumping energy requirements and pipeline length.

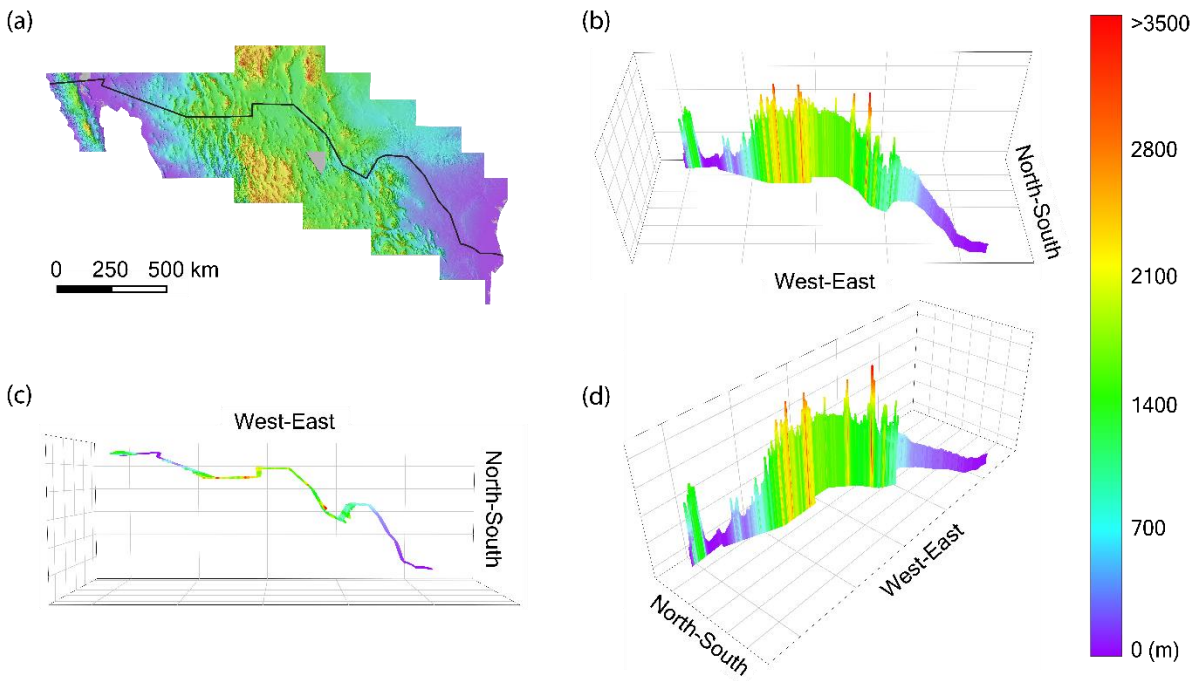

Figure 3-2: Topographical maps of the US-Mexico border are resolved using one-arc second (30m) resolution satellite-based Digital Elevation Models (DEMs) (a). The elevation profile of the border itself is extracted for visual reference and shown as (b) front-facing, (c) top-down and (d) side-view. Any grey in the heatmap profile should be taken as either missing data or below sea level (<0m).

Cumulative pumping power over the generated border profile was calculated by solving an iterative Bernoulli energy balance, accounting for head loss, while assuming constant pressure. The Darcy-Weisbach (eq. 3-1) and Swamee-Jain (eq. 3-2) models were used to formulate friction head loss (ΔH)[149]. Parameters for these models are: friction factor (f), pipe length (L), fluid velocity (V) and gravity (g), surface roughness (k), hydraulic pipe diameter (D_h), and Reynolds number (Re).

$$\Delta H = f\left(\frac{L}{H_d}\right)\left(\frac{V^2}{2g}\right) \tag{3-1}$$

$$f = \frac{1.325}{ln\left(\left(\frac{k}{3.7D_h}\right)+\frac{5.74}{Re^{0.9}}\right)} \tag{3-1}$$

For the material of the pipeline, concrete cylinder piping is selected and taken to have a surface roughness of 0.03 mm[150,151]. To keep the water velocity below the assumed maximum for the system (3 m/s)[152], pipes are sized at 54” (1.37 m) with either 8 or 16 pipes in series depending on desalination configuration. Eight are used if two desalination plants are deployed and 16 are used if only one plant is considered. Different materials and sizes were initially tested, and 54” concrete cylinder piping was found to be the most cost-effective option while satisfying the design and safety parameters.

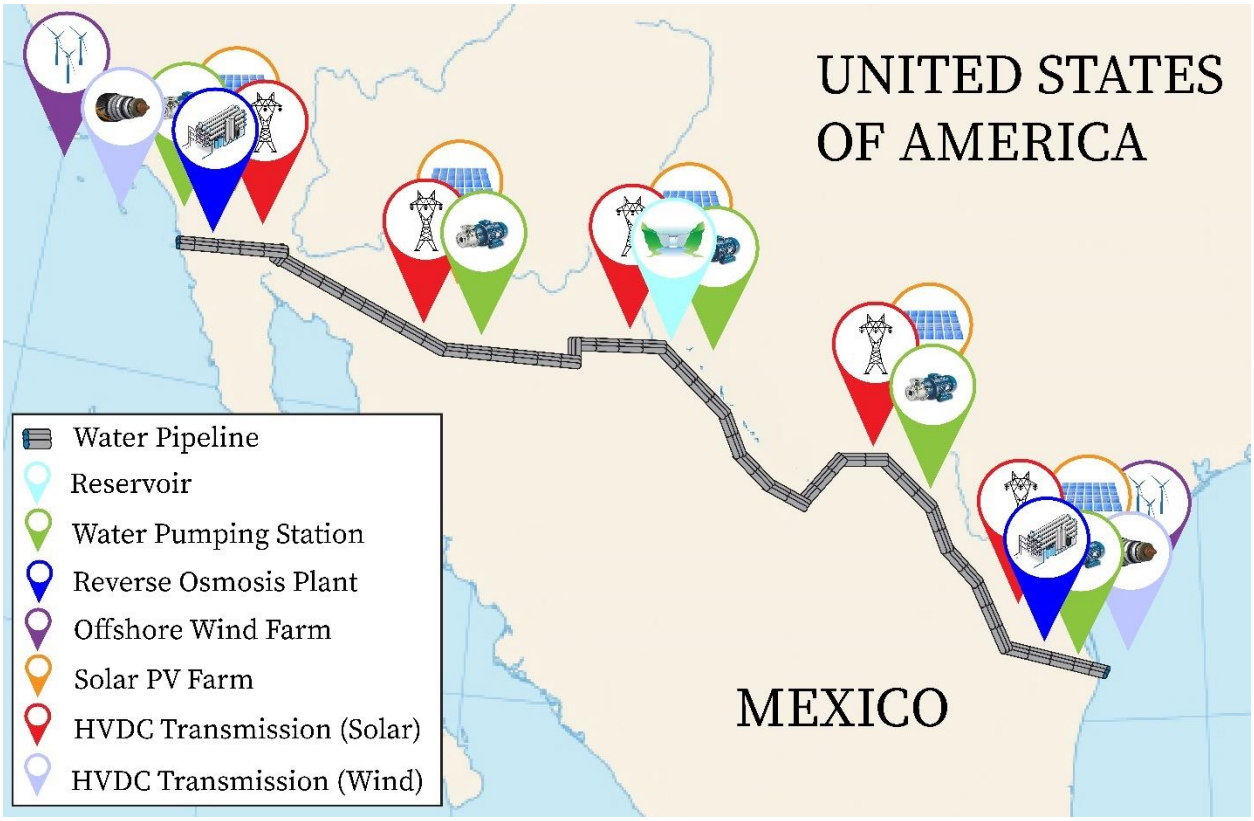

Figure 3-3: A sample design of the infrastructure for the dual reverse osmosis plant test cases. The pipeline signifies the evaluated route for water piping which parallels the border. Locations for the midway reservoir, pumping stations and desalination plants are displayed for visual reference. Note that the reservoir is located at the break-even energy location if water is pumped from either coast. Pins are not located precisely where technologies are deployed but rather are spread for visual convenience.

The border profile presented in Figure 3-3 indicates sites of interest consisting of desalination plants, pumping stations, solar/wind farms, transmission and a midway reservoir. The midway reservoir location is selected at the point where pumping loads from the east and west

coast become equal, about 713 MW cumulative from either side. The locations for the intermediate pumping stations were determined by the energy consumption from either coast to the midway reservoir. For either route, the pumping station was placed at the mean cumulative energy location from coast to reservoir, which was matched with its corresponding coordinates along the border. Additional pumping stations were accounted for at the coastal desalination plants and reservoir.

Table 3-1 shows the location of each of these points of interest as well as the cumulative pumping power to reach them from either side of the border. For transmission purposes, total terrain-adjusted distances from each pumping station to the nearest large population center (>250,000 residents) and respective PV farm are also given. The structure and characteristics of this inter-grid transmission infrastructure is described in Section 3.8.3.

Table 3-1: Presented are the locations of each pumping station along the border. Cumulative pumping loads from either side of the border assuming half of the water load is pumped from either direction. Distances from each pumping station to its respective PV farm plus the distance from each station to the nearest city are also given.

	Location 1	Location 2	Location 3	Location 4	Location 5
Longitude	32.54	31.41	31.41	28.25	26.00
Latitude	-117.12	-111.22	-106.06	-100.1	97.15
Cumulative Load (kW)					
West-East	0	420,346	712,459	819,960	919,038
East-West	924,323	861,780	712,456	267,233	0
Transmission Distance (km)	457.5	103.3	116.6	215.156	69.0

3.7 Desalination

Reverse Osmosis was chosen in the project over thermal processes due to its lower energy consumption per unit water produced, known as specific energy consumption (SEC)[111–114,153,154]. The process is performed by forcing water through a selective membrane at high pressure to separate salts from water. Figure 3-4 shows simplified designs of typical RO processes for three tiers of technological complexity and capital cost, which are used as reference in the analysis.

Figure 3-4: Three schematics of typical RO processes examined by this study, each displaying increasing efficiency, complexity and cost. Note that processes (b,c) often integrate process (a) into their systems to further increase efficiency. (a) Single/Mutli-pass reverse osmosis, where multi-pass describes feeding the brine outflow from the first membrane into additional membrane(s), in series, to increase the overall process recovery ratio (fraction of pure water produced to feed flow). Typical plants range from 2-3 passes before experiencing diminishing returns on efficiency. From left to right, saline feed water is pre-treated to balance the flow's pH and remove biological foulants, improving membrane longevity. Then the stream is pumped at high pressure through a membrane module, separating salts and other impurities from the outflowing pure water. Concentrated discharge is removed and disposed of. Post-treatment then reintroduces healthy minerals to the outflowing water for human consumption. (b) Almost identical to the previous process but includes some type of electrical or pressure exchanger (PX) recovery device to recycle kinetic energy in the brine outflow to increase overall process efficiency[155–157]. (c) An entirely different process of circulating water through the RO system traditionally described as semi/full-batch, where brine outflow is circulated back into the feed stream continuously using a circulation pump (semi-batch) or pumped into some type of pressure chamber and reused for the feed stream in discrete cycles (full-batch). The last two processes push the thermodynamic limits of Reverse Osmosis and full-scale plants are either infant in maturity (semi-batch) or lab scale (full-batch)[158–163]. While batch is still in development, it does provide the lowest theoretical energy consumption of any other known process.

Figure 3-4 continued:

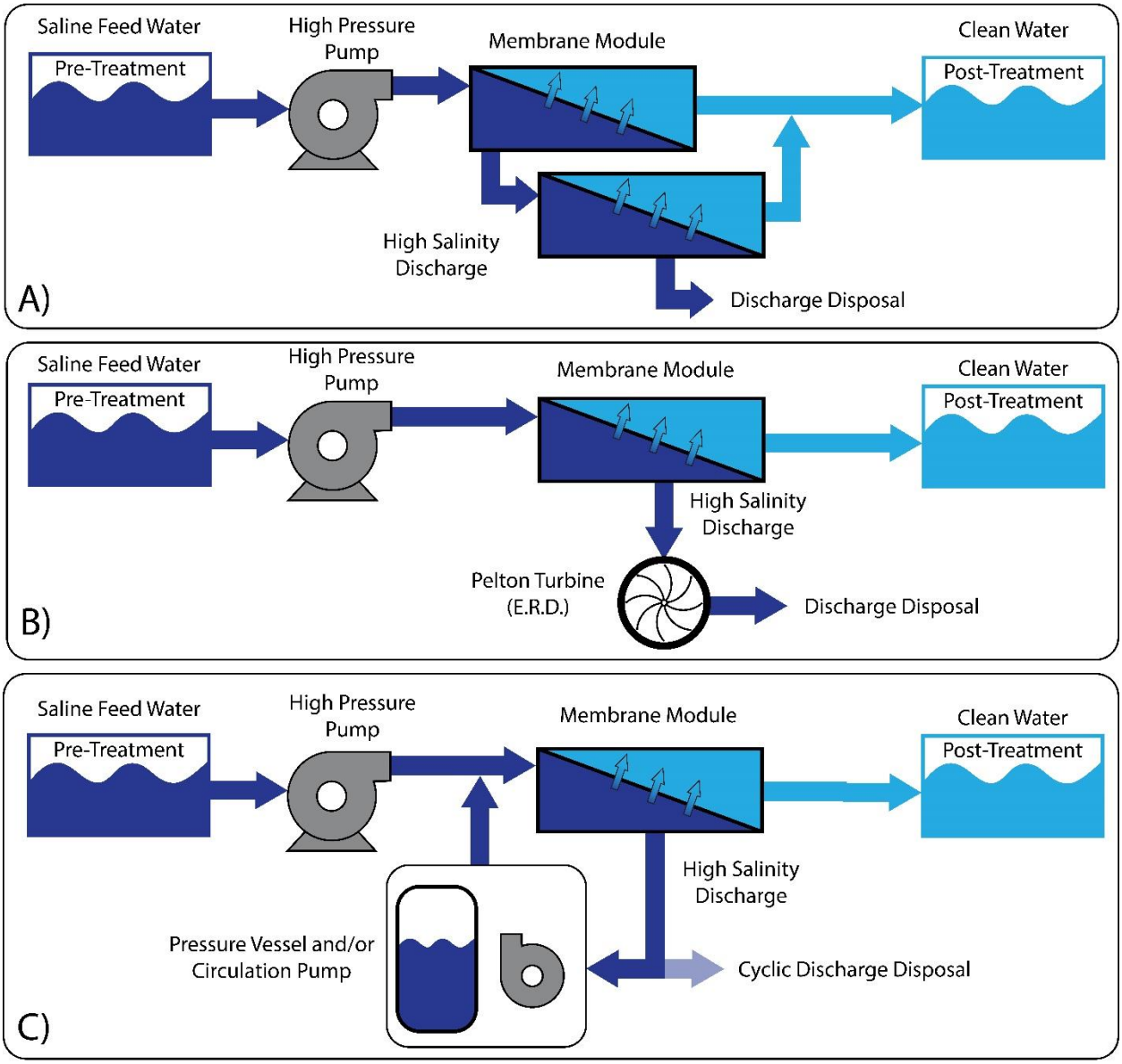

The chosen water production for the project was taken to be 1000 Mgal/day and plants were assumed to have a 96% annual availability, which is common for utility desalination facilities[111,112,114]. A design model breaking down desalination energy consumption by process component; pre-treatment, desalination, post-treatment and other minor processes, was used to calculate the energy requirements for the plants[112]. Three reverse osmosis technology categories were simulated to show a range of potential project configurations. Table 3-2 shows the specific energy consumptions for each tier of these technologies and their daily electrical load.

Pre-treatment of the feed stream is necessary to prevent early fouling of the membranes[164] and effluent brine must be responsibly handled to prevent environmental damage, which are all of consideration when designing a plant[153,165]. Irresponsible disposal of high salinity brine water can negatively affect the ecosystem around the plant[166,167]. Therefore, brine disposal was taken as top-of-the-line in environmentally friendliness, assumed to use large diffusers or similar technology, and was priced accordingly. The Carlsbad Desalination Plant in California, USA can provide an example of this type of discharge technology[167].

Table 3-2: Specific energy consumption (SEC) for the three categories of reverse osmosis technology, separated into the three tiers in represented in Figure 3-4[112]. Note that the SEC provided is the sum-total of all RO plant processes and auxiliary systems for a given technology, i.e. pretreatment, desalination, post-treatment, etc. The Current Typical category consists of the average U.S. energy consumption for RO as of 2016. State-of the-art is defined as the minimum SEC if the best available technologies are used and would encompass high efficiency processes such as those with inline energy recovery[155–157]. The practical minimum is defined as the lowest SEC one would see if the best R&D/theoretical technologies were employed. This category covers a wide range of new processes such as semi-batch and the more efficient full-batch RO[158–163].

RO Technology	SEC (kWh/m^3)	Daily Electrical Load (kWh)
Current Typical	3.69	13,960,000
State-of-the-art	2.95	11,160,000
Practical Minimum	1.70	6,420,000

3.8 Renewable Power Production Modeling and Inter-grid Transmission Infrastructure

Wind and solar energy can provide a recurrent source of electricity in a clean and sustainable fashion, with the added benefit of highly reduced operational water withdrawal over fossil fuel technology. Detailed in this section is the integration of offshore wind turbines and solar panels into the project's energy infrastructure. Studies show that U.S. coastal waters near the border experience high average wind speeds and harbor the opportunity to further expand the US offshore wind industry[18,121–123,168]. Similarly, the US-Mexico border interior contains some of the best solar resources in the world[127,137]. Sites around the Pacific and Gulf coastlines and along the border were evaluated for their wind and solar potential energy production capabilities. The necessary new electrical transmission infrastructure needed to deliver this power was also considered for cost purposes.

While the cost of offshore wind is more expensive in the US than in European countries, many believe that the US industry simply needs to build out its supply chain infrastructure to bring down costs. A project of this scale could initiate the much needed expansion of the supply chain[123,124,130]. The offshore economics presented in this study are meant to provide perspective on the potential technologies that can be implemented.

3.8.1 Wind

Wind Site Selection and Sub-Structure Characterization

Two regions of interest on the east and west coasts of the border were chosen for their wind resources and capability to power the RO plants, using NREL's WIND Prospector interface and Toolkit database[133–136]. These two coastal sites were selected for optimal average wind speeds and shallow depth. Ocean floor depths at these locations are of importance because the substructure supporting the wind turbines relies heavily on this parameter for design choice and cost estimation.

For this analysis, offshore wind technology was broadly categorized under two substructure types based on water depth, fixed-bottom, which are foundationally attached to the ocean floor, or floating, which sits atop a barge or buoy like structure[71,79,85,98,99,168–170]. Figure 3-5 shows a topographical map of both the Southern California and South Texas sea floor, built from data retrieved from the NOAA bathymetric database[171,172].

On the west coast, there is abundant wind off Santa Rosa Island, while the East coast benefits from desirable resources in direct proximity to the border. Due to the Southern California offshore bathymetry, which drops abruptly below 50m, floating offshore wind technology is the best option for the location around Santa Rosa Island. In the case of South Texas, the offshore depth is much more conducive towards fixed-bottom wind turbines. In the remainder of the analysis, each wind farm configuration will be treated according to their assumed sub-structure type.

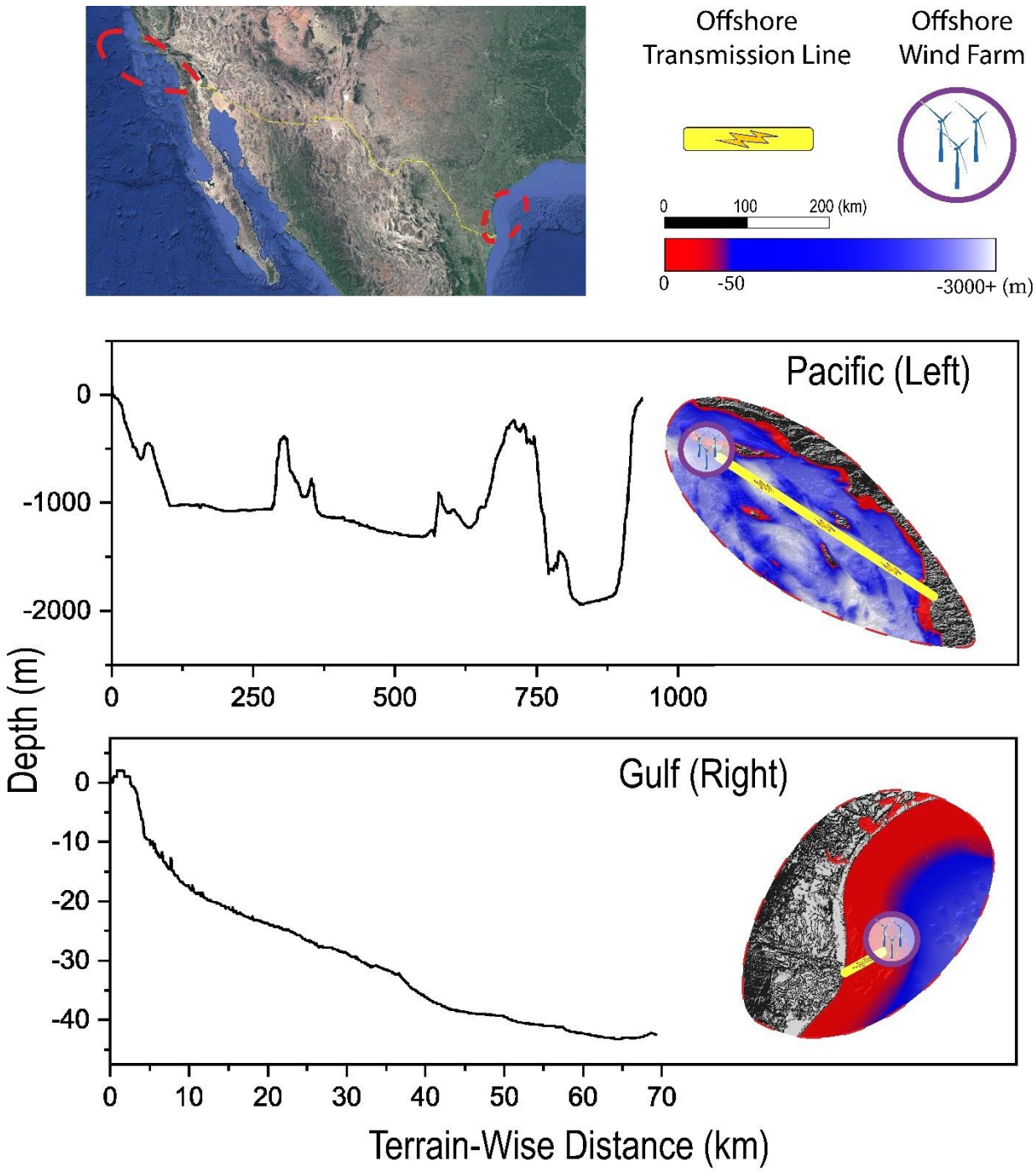

Figure 3-5: Topographical reliefs of the Southern California and Gulf ocean-floor with terrain paths, for transmission purposes (highlighted in yellow), from each desalination plant to its respective wind farm. Ranges on depth go from 0-50m (red), to 51-3000 (blue) then 3000+ (white)[171,172]. The red area indicates the region where fixed-bottom offshore technology can be employed and depths outside this region must use floating foundations.

Offshore Wind Transmission

Depending on the location of an offshore wind farm, electrical transmission can make up a large portion of the project's installed cost. Careful analysis of the bathymetric profiles of the ocean floor along the transmission route is critical in identifying cost and engineering complexities.

As shown in Figure 3-5, the majority of Pacific coastal seafloor is relatively deep, with many deep troughs and peaks along its length, increasing the difficulty of constructing this transmission line. The Gulf offshore profile is much more forgiving with a gradual slope and shallow depth. As with the border elevation profile, each transmission route was calculated based on the actual lateral distance traversed along the sea floor.

The type of transmission modelled in this analysis employs High Voltage Direct Current (HVDC) technology. HVDC technology has grown in popularity in recent years for its enhanced transmission efficiency, of roughly ~3%/1000km[173], over High Voltage Alternating Current (HVAC) at high power and long distances[174–176]. This both increases the overall power transfer capabilities of the transmission line and reduces the size of the wind farm needed to satisfy desalination.

Wind Energy Production

Unlike onshore, offshore wind generally has fewer constraints regarding size, and projects are routinely being built with higher capacity turbines. Since very little of the offshore environment is restricted by scale, this project was modelled with theoretical 10 MW wind turbines, as they are likely to be a future standard for offshore[16,17,177–180]. Parameters for the theoretical turbine were derived from an optimized model from Delft University and are given in **Appendix A**.

Hourly wind data was collected for Pacific and Gulf locations of interest from the NREL WIND Toolkit[133–136] and processed into weekly-hourly average velocities and standard deviations. The power produced by wind turbines at each site were calculated using eq. 3-3 with parameters: rotor area (A_{rotor}), referenced generator efficiency (η_{gen}), air density (ρ), the location's Weibull probability distribution ($Prob_w$), coefficient of power (C_p) and wind velocity (V_w). A full description of the model can also be found in **Appendix A**.

$$\overline{P_T} = \frac{A_{rotor}\eta_{gen}\rho}{2}\int Prob_W C_P V_W \, dV_W \qquad (3)$$

Table 3-3 shows the location of each potential wind farm site as well as the annual energy production (AEP) and Capacity Factor simulated for a single turbine at each site.

Table 3-3: Production and design properties for the simulated Pacific and Gulf wind farms. The coordinates of each farm and its respective distance to the proposed desalination plants are provided, as well as the simulated annual energy production and capacity factor at each location. Note the large terrain-adjusted distance for the Pacific transmission profile, mainly due to the frequent elevation changes and depth of the ocean floor in this region.

Location	Pacific	Gulf
Coordinates[133–136] Latitude Longitude	 26.93 -97.16	 33.67 -120.21
Terrain-Adjusted Distance to Desal Plant (km)	1747.24	71.16
Annual Energy Production (kWh)	39,230,000	34,980,000
Capacity Factor (%)	44.7	39.9

3.8.2 Solar

Solar Site Selection

Solar farm locations were dependent upon their corresponding pumping stations locations and were chosen to help minimize transmission loss/cost and maximize energy yield. Table 3-1, Section 3.5 shows the theoretical pumping station locations along the pipeline and were used as reference for determining solar farm locations. Table 3-4, Section 3.8.2, *Solar Energy Production*, shows the ideal areas for solar near these pumping stations, selected using NREL's National Solar Radiation Database (NSRDB).

The interior of the US-Mexico border has large amounts of undeveloped land and as such, it is easy to locate potential sites close to pumping stations. These interior sites were selected based on their location along the pipeline, proximity to large population centers and resource availability. The coastal locations are more populated and therefore farm locations were chosen further away from their pumping stations. In the case of California, the region near the coast is densely populated, therefore this solar farm must be located on the other side of a small mountain range to satisfy land requirements.

Solar Transmission and Grid Connection

The distance from each solar farm to its pumping station was calculated using the same terrain-wise method described for the border elevation and offshore transmission profiles. Solar installations along the interior of the border were easy to co-locate with their pumping stations, therefore PV farm to pumping station transmission cost was not addressed. In the case of the coastal locations, the farms are measurably far from their stations, requiring transmission lines to be added. Table 3-1 and Table 3-4 show where the pumping stations lie in comparison to the proposed PV farms.

While PV farms have a very low cost of energy, without accompanying storage power can only be provided during sunlight hours. As stated in Section 3.6, pumping stations have been outfitted with independent transmission systems that tie to the nearest population center. This ensures the pumping stations always receive power regardless of the hour and provides the added benefit of draining excess power from the grid when demand is scarce and supply is abundant.

Solar Energy Production

The ratio of a single panel's annual electrical output to its corresponding pumping station annual energy requirement is used to determine the number of solar panels required per farm. This method was applied for each solar farm location. Hourly global horizontal radiation data was gathered for each of the five sites in Table 3-4 from NREL's NSRDB for the year 2018. From here, the total incident radiation on a south facing tilted surface (I_T) was calculated using the Liu-Jordan model (eq. 3-4)[138,181,182]. Parameters for this model are: beam radiation (I_b), diffuse fraction (R_b), diffuse radiation (I_d), surface slope or tilt (β), total horizontal radiation (I) and ground reflectance (ρ_g).

$$I_T = I_b R_b + I_d \left(\frac{1+\cos(\beta)}{2}\right) + I\rho_g \left(\frac{1-\cos(\beta)}{2}\right) \tag{3-4}$$

The ratio of atmospherically reflected to direct incident radiation, or diffuse fraction (R_b), for each solar farm location was estimated from the NSRDB data using the Erb's Correlation (eq. 3-4)[183] with local clearness indexes (k_T).

$$R_b = \begin{cases} 1.0 - 0.09k_T & for\ k_T \leq 0.22 \\ 0.9511 - 0.1604k_T + 4.388k_T^2 - 1.638k_T^3 + 12.336k_T^4 & for\ 0.22 < k_T \leq 0.8 \\ 0.165 & for\ k_T > 0.8 \end{cases} \quad (3\text{-}5)$$

A similar analysis was run with an East-West single-axis solar tracking surface. The solar radiation electrical output was calculated from a reference panel using traditional electrical conversion equations which take radiation levels and cell temperature into account. A full description of equations and parameters for this model can be found in **Appendix B.**

Each pumping station site was evaluated with a range of surface tilts to determine the optimal slope for peak energy production. A 450W SunPower solar panel was used as a reference to estimate the practical electricity production of a single panel for each site. Operating conditions for the panel can be found in **Appendix B.** Output optimal fixed tilt angles, annual energy production for both a fixed and single-axis tracking models and capacity factors for each farm are shown in Table 3-4. Section 3.9.3, *Solar Farm Costs (Installed & O&M)*, contains a table depicting how much land area must be allocated to each solar farm.

Table 3-4: A breakdown of each Solar PV farm location and its respective energy production given a fixed tilt or single-axis tracking solar panel. Fixed tilt slopes were optimized for each location to produce the most energy. The first term in capacity factor corresponds to fixed tilt panels and the second corresponds to single-axis tracking.

	Coordinates	Optimal Tilt (deg)	Annual Energy Production (kWh)		Capacity Factor (%)
	Lat-Long		Fixed Tilt	Single-Axis Tracking	
Farm 1	(32.73, -116.3)	26	909.440	974.923	23.1-25.7
Farm 2	(31.41, -111.22)	27	884.303	980.010	22.4-24.9
Farm 3	(31.57, -106.06)	26	905.175	978.863	23.0-24.8
Farm 4	(28.25, -100.1)	21	888.576	980.955	22.5-24.9
Farm 5	(26.01, -97.42)	17	727.287	809.955	18.4-20.5

3.8.3 Inter-Grid Transmission and Power Purchase Agreement Considerations

Transmission to each pumping station and desalination plant is crucial because renewable energy technologies only generate power while resources are available. To ensure that pumping stations receive power regardless of meteorological conditions, HVDC cabling was used to connect each station to a highly populated region (>250,000 residents). This cabling enables the dynamic buying and selling ecosystem that would satisfy pumping and desalination loads when on-site renewables are unavailable.

For economic purposes, Power Purchase Agreements (PPAs) can be used to both sell excess production and acquire power when needed[16,21,168]. The value of the PPAs can be inferred by the LCOE produced by each renewable installation and may even generate profit to offset operation and maintenance costs and the initial investment. Real-time energy prices are generally higher than average during the morning and late afternoon, therefore excess solar/wind power from the oversized systems can be sold at a premium. Nighttime demand usually has below average prices so energy bought back during this time would be financially beneficial[184,185]. It is important to note that these hourly pricing profiles change drastically based on the season, region and energy mix of different service providers. Although PPA's provide a promising source of economic benefit, they are not considered in the current analysis.

3.9 Cost Modeling

3.9.1 Project Versions

To cover the wide range of designs that this project may take to achieve optimal economics, 3 major configurations of the piping and desalination structure were considered. The first two being if the desalination plant was sized to meet the total water requirement along the border and placed solely on the west or east coast. Pumping was scaled by adding extra pipes so that physical fluid properties did not change. The third configuration was if the water production was split between the east and west coast and pumped inland from both sides. A total of 108 renewable project variations were analyzed using high, low and average installed costs for infrastructure and the Levelized Cost of Electricity (LCOE) (eq. 3-6) and Levelized Cost of Water (LCOW) (eq. 3-7) of each case is reported.

LCOE is calculated using the capital recovery factor (*CRF*), initial capital cost of the power generators (renewable/fossil fuel) (*ICC*), fixed and variable operation and maintenance (OM_{fixed}, OM_{var}) and total annual energy produced (E_{tot})[32]. LCOW is calculated in the same fashion but divides costs by the total water produced (W_{tot}) instead of electricity, the initial capital cost encompasses the entire project infrastructure and variable operation and maintenance is reparametrized for water production using specific energy consumption (SEC).

$$LCOE = \left(\frac{CRF*ICC+OM_{fixed}}{E_{tot}}\right) + OM_{var} \tag{3-6}$$

$$LCOW = \left(\frac{CRF*ICC+OM_{fixed}}{W_{tot}}\right) + OM_{var} * SEC \tag{3-7}$$

The variations were categorized as follows: 3 different desalination processes sized for the same production capacity, each covering a unique specific energy consumption. For each of these variations, 4 pairs of wind and solar PV technology were used to satisfy the electrical loads of the three system configurations stated above. Thirty-six of the renewable variations were calculated using only solar technology to test differing economics.

To validate the sustainability of the project, an additional 27 comparative versions were simulated that replace renewables with two versions of natural gas technology as well as grid purchased electricity. A flowchart is given in Figure 3-6 to visualize the organization of the project version methodology. Further detail on these versions can be found in the remaining sections.

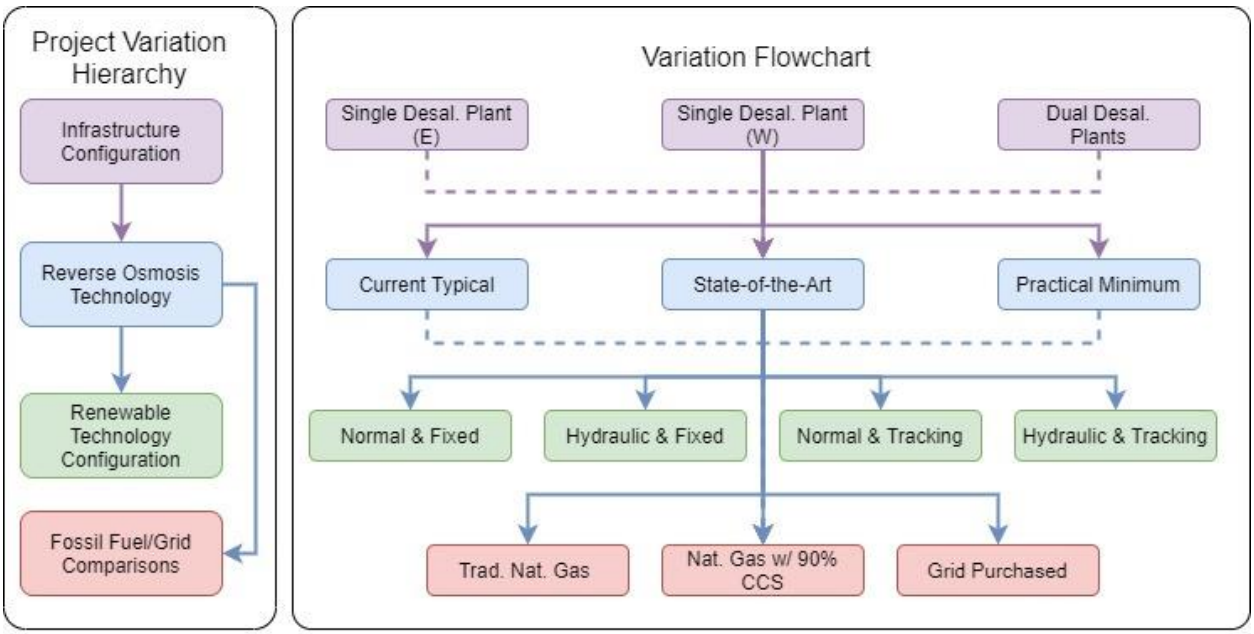

Figure 3-6: A flowchart visualizing project variation organization with hierarchy design (left). The structure (right) has been broken down into three desalination infrastructure configurations, defined as the location of the plant(s). Each of these configurations includes three different reverse osmosis technologies. Finally, each of those tiers were evaluated with four different combinations of renewable energy for electricity requirements. Three comparative sources of energy, from fossil fuel or grid electricity were also tested in place of renewables. Solar only variations have been omitted for visual convenience. Note that nodes producing dotted flows follow the same directional hierarchy as solid flows.

Table 3-5 provides an itemized list of cost estimates used for the various parts of the project. Wind and solar installed costs were recorded from reference studies as averages, but a ±10% range has applied to encompass practical market fluctuations.

Table 3-5: Itemized installed and operation and maintenance (O&M) costs are provided for each portion of the project with either a high and low or average value. Each underlying component is given with their respective units for calculating total expenses. Fossil fuel calculations include a variable (unforeseen) O&M component, recorded as the second term under O&M expenses (a). Wind farm costs are calculated with respect to their designed configuration (floating or fixed bottom) and drive-train type (traditional or hydraulic). Grid electricity only considers the fixed capital cost per unit energy in calculations and only includes transmission as described for solar farms and pumping stations. Desalination costs are shown for Current Typical plants only. State-of-the-Art and Practical minimum installed costs are assumed to be 10 and 20% extra accordingly but O&M expenses are kept the same. A special note for the HVDC converter is all project variations use this range for cost estimates except for the East or West coast only configurations for Current Typical desalination, which use the range ($106-113 mil) to account for larger HVDC converters. Under pipeline, trenching and excavation as well as embedment, backfill and compactification are abbreviated as T&E and EBC.

Table 3-5 continued:

Component	Units	Installed Expenses		O&M Expenses	
	(Installed)-(Fixed O&M)-(Variable O&M)	Low	High	Low	High
Wind Farms[30,186]	($/kW)-($/kW/yr)				
Fixed-Bottom (Trad.)		3999	4888	129	
Floating (Trad.)		4820	5891	137	
Fixed-Bottom (Hyd.)		3412	4170	129	
Floating (Hyd.)		4112	5026	137	
Solar Farms[21]	($/Wdc)-($/kW/yr)				
Fixed Tilt		0.954	1.17	9.1	
Single-Axis Tracking		1.02	1.24	10.4	
Fossil Fuels (Nat. Gas)[20]	($/kW)-($/kW/yr)-($/MWh)				
CC gas w/ 90% CCS		2569		27.48-5.82[(a)]	
Multi-shaft CC gas		954		12.15-1.86[(a)]	
Grid Electricity[187]					
Average Industrial Price	(¢/kWh)	6.50			
Desalination[153]	($/m^3)-($/m^3/yr)	1,470	6,005	0.16	0.385
Transmission[169,188]					
Wind Farms					
HVDC Converter	(mil $ per)	81.0	99.4	N/A	
Cable Systems	($/m)	403	403	N/A	
Offshore Platforms	(mil $ per)	9.94	13.7	N/A	
Cable Installation	($/m)	373	869	N/A	
Solar Farms					
600 kV HVDC bi-pole	($/m)	1202		N/A	
Pipeline[150]					
Base Pipe	($/m)	449		N/A	
T&E	($/m)	55.8		N/A	
EBC	($/m)	36.1		N/A	
Pumping Stations[189]	($/kW)	175	350	N/A	
Reservoir[190]	($/ML)	1278		N/A	

3.9.2 Infrastructure Costs

Water Pipeline, Pumping Stations, Reservoir

Based on a reference study, the water pipeline is sized for each configuration with a constant diameter of 54" [150]. Concrete cylinder piping was found to be the most cost-effective material while satisfying the design requirements. Parameters for the pipeline cost model are the pipeline itself, trenching and excavation (T&E), assumed as sandy gravel soil with 1:1 side slope, and embedment, backfill and compaction (EBC), which are assumed to be ordinary in the context of the model.

A reference study covering hydro-electric storage is used to estimate the cost of pumping stations[189] due to their shared use of large water pumps[146]. Standard hydro projects allocate ~35% of installed costs to equipment, of which 50% is assumed to contribute to a pumping system.

The reservoir cost is estimated from a reference study[190] quoting cost, based on capacity, which is 180,000 MGal (681.3 Mm^3) + 5% dead volume. Reservoirs are low volume, designed to order projects, so cost models cannot be entirely confident for extrapolated predictions. Estimates provided in this analysis may vary slightly from what is found in practice.

Wind and Solar Transmission

Installed electrical transmission costs for the project were estimated based on two key parameters: length of line and line capacity. Auxiliary components were determined and priced based on these characteristics. Wind farm transmission lines were modeled as subsea HVDC cabling**.** System components were a 500 MW 300 kV HVDC converter, auxiliary cable systems, jacketed offshore DC platform and single trench, single cable installation[169]**.** Solar transmission costs were slightly less detailed and only accounted for 600 kV HVDC bi-pole caballing and installation[188].

Desalination

Desalination costs were broken down by internal process using a reference design report[153]. Capital costs have been kept as in the reference study except for concentrate disposal and waste and solids handling which are taken as $50-750 and $20-180 respectively to account for

environmentally friendly brine disposal. For each RO technology, Typical, State-of-the-art and Practical Minimum, assumed capital costs multipliers of 1, 1.1 and 1.2 have been applied respectively.

3.9.3 Renewable Resource Costs

Wind Farm Costs (Installed & O&M)

Wind turbine installed costs were based on the rated capacity for the project and have been split into two categories, hydraulic and traditional transmissions. Wind turbine technology has been maturing for several decades and steadily decreasing in cost[130,186,191]. Novel configurations and components continue driving down costs even further such as the usage of a hydraulic drivetrain in place of a traditional gearbox[26,27,59,60,63,64]. This alternative has shown promise in a variety of demonstration projects and may lower the cost of offshore wind by a sizeable amount [30]. Estimates for this hydraulic turbine are calculated by applying reduction projections[30] to traditional turbines from an NREL report[186]

As stated in 3.8.1, *Wind Site Selection and Sub-Structure Characterization*, the Gulf portion of the project employed fixed bottom offshore wind turbines, but the Pacific side has been restricted to floating platforms. The different costs (installed and O&M) associated with these sub-structure designs were derived from an annual NREL report [186]. Table 3-6 gives the number of turbines in each location for different desalination technologies.

Table 3-6: Wind turbine size requirements to meet desalination loads, separated by major project configuration and desalination technology. Note that the single plant section refers to the total number of turbines in each location, while dual plants must be summed across Pacific and Gulf to return the total.

Project Location	Pacific	Gulf
Number of Turbines		
Single Plant		
Current Typical	129	141
State-of-the-Art	103	112
Practical Minimum	60	65
Dual Plants		
Current Typical	65	71
State-of-the-Art	52	56
Practical Minimum	30	33

Solar Farm Costs (Installed & O&M)

Like for wind turbines, the cost of utility scale solar PV projects has drastically declined, hitting record lows that rival if not eclipse fossil fuel in the right conditions[21,130,192]. The three dominant technologies for traditional utility scale systems are fixed tilt, single-axis and two-axis tracking. While two-axis tracking is guaranteed to produce the highest production per panel, the added cost of the equipment rarely makes it desirable over single-axis trackers, so two-axis trackers were excluded from the analysis. NREL Benchmark[21] reports were used to determine the installed and O&M costs for both technologies. Table 3-7 reports the number of panels, adjusted for transmission losses, and the minimum land area required per location.

Table 3-7: Transmission loss adjusted number of panels for each farm to meet its respective annual pumping load, simulated for optimized fixed-tilt and one-axis tracking systems. Land areas give a low-end estimate of the space required to construct each farm, only accounting for total panel surface area.

PV Farm Size and Scale

	Fixed Tilt		Single-Axis	
	# of Panels	Land Area (km^2)	# of Panels	Land Area (km^2)
Farm 1	4968184	10.04	4640694	9.38
Farm 2	4883133	9.87	4405654	8.91
Farm 3	5261405	10.64	4504758	9.11
Farm 4	8430416	17.04	7636290	15.44
Farm 5	3106431	6.28	2790777	5.64

3.10 Fossil Fuel and Grid Produced Electricity Test Cases

To give perspective on why renewables are beneficial for the project, 27 additional project variations encompassing combined cycle natural gas with 90% carbon capture and storage (CCS), multi-shaft combined cycle natural gas and grid purchased power, have been included in the final levelized cost of water results[20]. Combined-Cycle with 90% CCS is the role model in low emission natural gas and a fossil fuel direct competitor with renewables in terms of green energy concerns. Multi-shaft combined cycle plants are some of the cheapest forms of natural gas energy but emit pollution, unlike renewables. The last comparison case assumed that no power production facilities were constructed, and only grid electricity was used and bought at market price.

Pumping and desalination loads were satisfied by fossil fuel plants in these comparisons. Transmission on the coasts was omitted due to the assumption that fossil fuel plants were co-located with desalination plants, however grid connection to the nearest large population center was retained. For the case of grid purchased electricity, the same procedure was used with no allocation for power production, and the price of power was assumed to be the average of the industrial sector[187].

3.11 Emissions, Water Withdrawal Averted During Energy Production and Labor Contribution

Although renewables provide a wealth of advantages over non-renewables, the major benefit traditionally referenced is their reduction to global emissions. It has been widely shown that wind and solar power have very low direct/indirect emissions over their lifespan, whereas non-renewables have produced enough carbon dioxide to considerably contribute to global levels[11,193]. As discussed above, the goal of the project was to provide sustainable water to the US-Mexico border, where "sustainable" encompasses environmentally responsible electricity usage.

Another advantage of renewables over non-renewables are their low water use during operation[139]. When coupling any water purification technology to an energy source, a major consideration must be the quantity of water that is withdrawn to produce that energy. As the interior of the border is already exhausting its natural water resources, using non-renewables for the project infrastructure would only exacerbate the situation.

While environmental factors are widely cited in the argument of renewables over non-renewables, often forgotten is the larger labor contribution that these technologies provide to the economy. Studies show that renewables are not only outperforming their counterparts in terms of financial economics, but also providing much higher levels of job creation[139]. Table 3-8 shows the metrics used for calculating the benefits, discussed above, that this project can provide if renewables are considered.

Table 3-8: Metrics for calculating sustainability impacts of different energy generation technology. Water withdrawn describes the total water drawn from surface or groundwater sources, not the water consumed during operation[139]. Emissions reported reflect the total CO2 and CO2 equivalent pollution emitted by the technology over its entire life cycle (construction/manufacturing, operation and decommissioning)[194–198]. The jobs added reflect current data on each industry and account for supporting roles such as supply chain and sales[139].

Technology	Water Withdrawal (m^3/MWh)	Emissions (tonnes CO_2/GWh)	Jobs Added (#/GWh)
Natural Gas	1459	450	0.06
Wind	0	11	0.45
Solar	3.79	40	6.65

3.12 Results and Discussion

Without obtaining water security, the US-Mexico border region will only become more impacted by shortages and economic tension. This analysis presented a concept for achieving this security in a sustainable fashion using renewables and saltwater desalination. By constructing this concept, a tangible value can be placed on the cost of producing this water and providing it to the region. The following sections discuss levelized cost analyses and a sustainability report.

Levelized costs were calculated with an interest rate of 3%[16,21,199,200], which represents an average range of federal, state and private funding opportunities over the project lifespan of 30 years. Installed costs and LCOW graphs are grouped by different desalination technology. The combination of wind and solar technologies used were grouped as: Hydraulic & One-axis (Tracking), Normal & One-Axis, Hydraulic & Fixed and Normal & Fixed. Section 3.12.1 gives the installed cost breakdown for each project variation. Levelized costs for electricity generation ranges for each solar and wind technology, averaged across every site, are given in Section 3.12.2. The full levelized cost of water for all variations, including a comparison with fossil fuel-based versions of the project and average domestic water prices, is shown in Section 3.12.3. Additional analysis covering emissions, water withdrawal averted and jobs added are presented in section 3.12.4.

3.12.1 Installed Project Costs

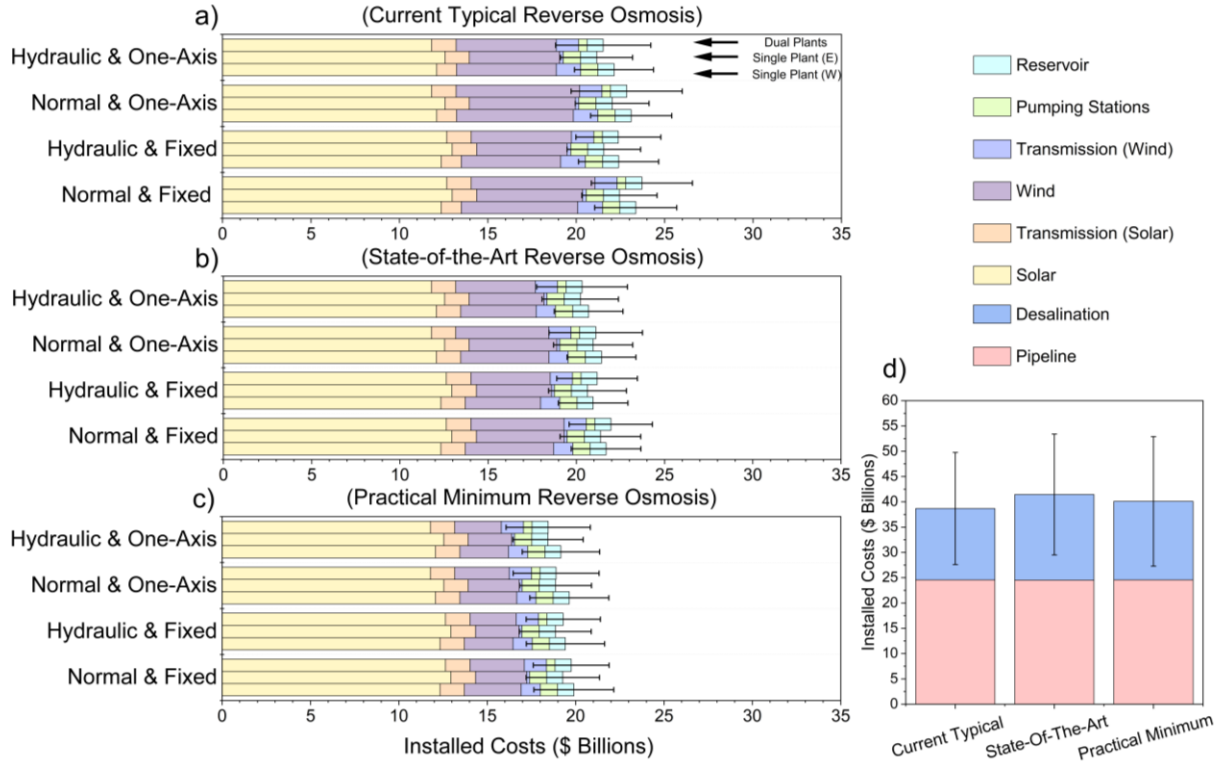

Figure 3-7: Total installed cost breakdowns for each variation using both wind and solar are shown above. The three major graphs (a-c) were split based on the desalination technology used. Within each desalination graph, variations have been split into four major groups by the renewable energy used for that case. Within each of those four categories are the three different desalination infrastructure configurations. From top to bottom the configurations describe if there are two RO plants (Dual Plants), one plant in the east (Single Plant (E)) or one plant in the west (Single Plant (W)). A separate graph is given to the right (d) and covers the pipeline and desalination costs for each RO technology type. These costs do not change between each RO category and are separated due to their high cost. To calculate total installed costs, pipeline and desalination costs should be added to their other respective RO technology category.

Figure 3-7 shows the average installed cost breakdowns, by major infrastructure configuration, for each wind and solar technology combination. Note, the cost drivers in every case were the pipeline infrastructure, solar and wind farms and desalination plant(s). The reservoir, pumping stations and transmission played a much smaller role in the upfront cost of the project.

The pipeline is purely a material and labor cost so economies of scale may shrink this expense considerably. Since the project requires at least 2800km of pipeline as designed, manufacturing rates will most likely be negotiated. While optimizing the pipeline for a lower elevation route could lower line losses and pumping power, additional piping costs needed for

these routes may outweigh the reduction to the solar farms. However, specific optimization of this relationship may yield an optimal route that is both cost and energy efficient.

Wind and solar both play considerable roles but are comparable to, if not outperform, fossil fuels and other alternatives in upfront costs. The much larger contribution of solar over wind can be explained by the pumping energy loads, which are 4-8x greater than that of desalination depending on the process efficiency. This means proportionally more solar capacity was installed. Desalination costs are also likely to decrease over time as newer and more efficient, technology, such as batch reverse osmosis, is adopted into mainstream markets [154,158–161,201]. Given the size of the plant(s) in this concept, economies of scale and continued innovation are likely to help decrease upfront expenses as well.

3.12.2 Levelized Cost of Renewables

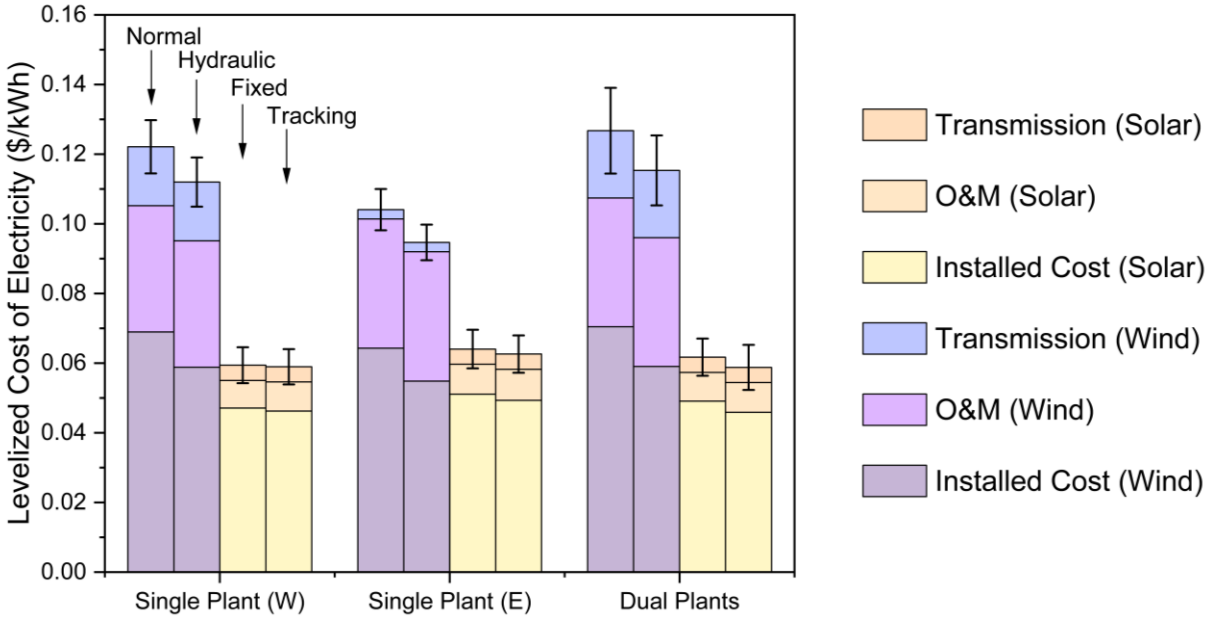

Figure 3-8: Levelized cost of electricity ranges for the project's wind and solar farms, averaged across each desalination technology category and between each farm. Offshore wind turbines were taken as traditional (normal) and hydraulic drive train. Solar panels were taken as fixed tilt or single-axis tracking. Levelized cost estimates are broken down by transmission, installed cost and operation and maintenance costs over the lifespan of each system.

Figure 3-8 shows the LCOE, based on eq. 3-6, generated by each renewable technology variation. Transmission for each farm has been included in the calculations as it was assumed to be necessary for the sale of excess electricity. Clearly the cost of offshore wind energy is much more expensive then solar. However, it is difficult to compare solar costs in this region with wind since the levels of radiation are some of highest on earth, producing extremely favorable economics. The US is also a much more favorable economy to develop solar over offshore wind due national supply chain differences. The U.S. offshore wind industry is less infrastructurally mature then utility scale PV, in terms of manufacturing supply chains and operational upkeep.

Wind's higher price is partially due to its relatively expensive O&M cost share, which is over 10 times more than solar in unit expenses. Wind lessens this gap with a much higher capacity factor, allowing it to generate more electricity per unit installed kilo-Watt. As the market for offshore wind continues to grow, future installed and O&M costs are expected to fall within global ranges. European wind costs are even lower than the global average and show a promising future

for the US offshore wind industry[130]. O&M, in particular, could decline by as much as half of the amount used in this study, heavily reducing the LCOE gap between wind and solar.

As mentioned in earlier sections, dynamic selling and purchasing of power will be necessary to ensure 24-hour operation. While the price of wind power makes it difficult to generate profit to supplement project costs, there is still a niche market for high cost PPAs, especially with independent system operators and industrial entities. The solar portion of the project provides a much more economically friendly source of income by contrast. Electricity prices vary widely around the country, but domestic sales are almost always in excess of the cost shown above[187]. Therefore, it is possible to generate extra income to reduce the overall cost of water produced.

3.12.3 Levelized Cost of Water

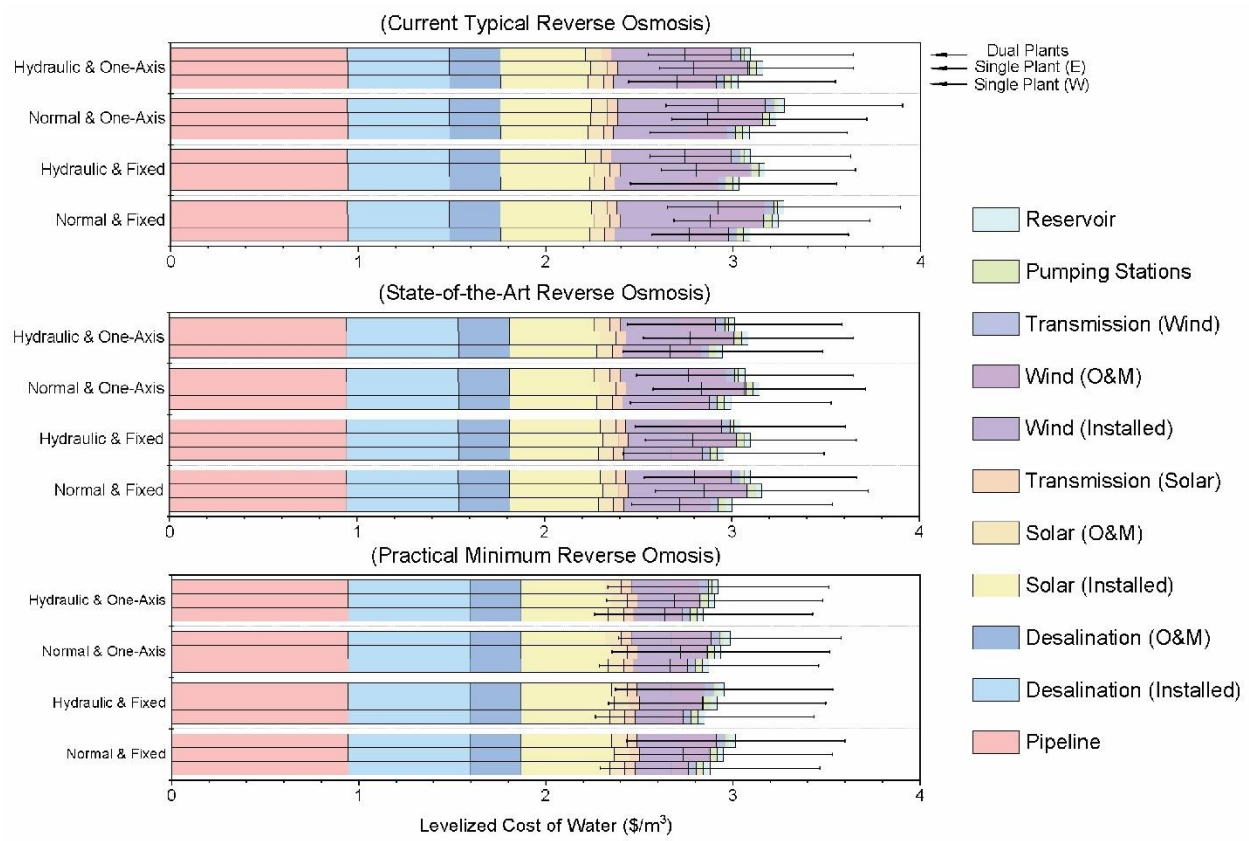

Figure 3-9: Ranges for the levelized cost of water are calculated for the three RO technology tiers and are further grouped by the four renewable technology combinations used. These four subcategories are split into three more groups describing whether there are two plants (Dual Plants), a single plant in the east (Single Plant (E)) or a single plant in the west (Single Plant (W)). Variations using only solar energy (not shown) yielded costs of 2.02-3.12, 2.02-3.17 and 2.00-3.21 ($/m3) for each RO category. Ranges for the cost of fossil fuel/grid produced energy are (not shown) calculated as 1.66-2.84, 1.66-2.88 and 1.66-2.95 ($/m3) for each RO technology category. A comparative price range for municipal domestic water is (not shown) found to be $0.27-1.87/m3, across a study of selected US cities[110]. Cities close to the border tended to fall on the high end of this range.

Figure 3-9 shows the levelized cost of water produced by each of the 72 variations. Included in the caption is the range of levelized costs that solar only configurations can achieve. Results for fossil fuel plants or grid electricity are also given with the upper end being state-of-the-art, low emission, combined-cycle gas plants with 90% CCS and the low end being either grid purchased energy or “dirty” combined-cycle multi-shaft plant produced electricity. The cases

presented above show a highly competitive levelized cost of water with the next leading "clean" fossil fuel technology.

The variations including solar only configurations show even more promising economics with LCOW ranges of \$2.00-3.21/m^3. These variations are roughly 10% less than those including both solar and wind but come with their own caveats. Integrating solar and wind helps smooth the intermittent power generation each experience and allows for a more homogenous energy profile that the grid can support. In terms of economic markets, wind is lagging behind solar in the US. By allocating a portion of this high value project to wind, a Keynesian economics "priming-the-pump" approach can be considered, which would bring down the cost of wind energy across the US. If only solar power and its lower raw costs are considered, then the grid may suffer, and the wind industry will lose out on a major financial injection for building out its infrastructure.

While the ranges of water cost presented for the project surpass those reported for select cities around the US[110], which are anywhere from \$0.27-1.87/m^3, the border states that would benefit from this concept usually fell under the high end of this spectrum, indicating increased economic viability. The water for this project was not anticipated to be entirely competitive with locally sourced water, given the cost of infrastructure required for desalination and delivery. However, the size gap between existing water pricing regimes and those calculated suggest that further cost refinement and income from future energy sales may allow the project to provide water at a price competitive with current infrastructure.

3.12.4 Emissions, Water Withdrawal Averted and Jobs Added by Project Configuration

Greenhouse gases in the atmosphere are reaching historic levels, prompting the uneasy thought that humanity will overshoot its goal of a <2ºC temperature rise, outlined by the Paris Agreement[202]. The creation of electricity greatly contributes to these rising levels, further grounding the argument for renewables which produce power with ultra-low life-cycle emissions. Table 3-9 shows the carbon dioxide emissions that each project configuration produces. Over the operational lifespan of the system (30 yrs), using solar and wind can avert producing anywhere from ~230-260,000,000 metric tons of carbon dioxide compared with natural gas, depending on the desalination technology used. This is not a miniscule amount of emissions, equivalent to ~1.7-1,900,000 cars[203], and should be taken as a major factor in considering the best energy system

to employ. Designing this conceptual infrastructure with renewables in mind would enable every energy intensive component to be satisfied while causing no further harm to the environment.

As stated before, withdrawing water for operating a power plant which is used to clean water is neither efficient nor sustainable when renewables are viable. When the water from thermal power plants is released back into the local supply, it often carries undesirable characteristics such as high heat. This can seriously harm local river and wildlife ecologies. While renewable variations withdraw ~61,000 m^3/yr over their lifespan, natural gas configurations heavily eclipse this, with ranges of ~27-31,000,000 m^3/yr withdrawn over the same period (Table 3-9). This is the equivalent to ~65-75,000 US households worth of water withdrawal annually[204]. These results are orders of magnitude apart and demonstrate the ecological and sustainable benefits that renewables have over natural gas.

A comparison of job creation between wind and solar vs. natural gas shows the same relationship as above. There is a clear argument for renewables over their counterpart, evidenced by the number of jobs solar and wind can add over natural gas. While natural gas may produce anywhere from ~11-1300 additional jobs, solar and wind provide orders of magnitude more at ~108-109,000. While the group expects the solar contribution to be over-estimated due to economies of scale not accounted for in the underlying data, it is an indicator of the massive potential that renewables bring to the economy. In particular, jobs will be created along the border, injecting the local economies with a much needed labor and financial boost. If the project is expanded to provide water infrastructure to both sides of the border, then this level of job creation could stimulate renewed growth in the region.

Table 3-9: Water withdrawal averted, Life-cycle CO2 emissions and jobs created over the project lifespan are calculated for each technology evaluated. Note that wind and solar must be summed to calculate the total contribution from a renewable only configuration. Wind is reported as having no water draw through its operation, but solar panels must be washed semi-regularly.

Technology	Water Withdrawal (Thousand m^3/yr)	Emissions (Mtonnes CO_2)	Jobs Added
Natural Gas	27-31,000	250-280	1,100-1,300
Wind	0	0.773-1.70	1,000-2,300
Solar	61	19.0	107,000

3.13 Limitations and Future Considerations

Limitations and challenges were frequently encountered, and the complexity of the project makes it difficult to develop an optimization scheme. Initial costs for the pipeline may be reduced by simplifying the route taken, however it is not immediately apparent whether this will drive up the pumping requirements satisfied by PV farms.

Further limitations were found when modeling the desalination plants. Since cost data on state-of-the-art and practical minimum technologies is not readily available, it was impossible to determine how they may completely affect the economics beyond lowering the SEC.

Transmission costs may be minor compared to the rest of the project, but this infrastructure is immensely important to satisfying project requirements and grid resiliency. The model of these systems used in the study falls short of a practical system design and the group intends to further refine its parameters. This will bring down the cost of transmission for offshore wind farms.

Another major technology discussed in the analysis was modular pumped-hydro storage. While the infrastructure only accounts for water storage, the potential for this technology goes well beyond just providing water security. Electrical grids are susceptible to fluctuations in stability and these hydro storage sites may be able to provide load balancing and baseline generation across a wide region of the country. In addition, these reservoirs can be sized in such a way to create a nationwide hub for excess energy storage, as an alternative to curtailment. These phenomena and the economics around using storage to take advantage of high price electricity sales are likely to be included in future work.

While interest rates are a key driver in infrastructure cost, this parameter was not analyzed in depth. Interest was assumed to be 3%, which while lower than commercial rates, is much higher than government financing. Simulations exploring financing indicated significant reduction to the LCOW in each project variation, enough to become competitive with inexpensive municipal sources. Renewable tax incentives are also not considered which would further lower costs.

3.14 Conclusion

Water usage along the U.S.-Mexico border has been shown to exceed what the local resources can supply. This causes sociopolitical and economic stress across the US and Mexican regions along the border through dry riverbeds and wells. Without adequate planning, the natural

water in the area will continue to unsustainably deplete. The above analysis presents a range of potential configurations for water security infrastructure along the U.S.-Mexico border. One-hundred eight renewable and 27 fossil fuel/grid variations were tested for their economic viability and sustainability impacts and grouped by different desalination technologies. Each of the three major configurations, utilizing one plant on either the east or west coast, or one on both coasts, show a range of costs competitive to those produced if "clean" fossil fuel technologies were employed. Configurations using both solar and offshore wind produce LCOWs of \$2.20-3.42/m^3, as compared to \$1.66-2.95/m^3 which was produced by fossil fuel plants or grid power purchasing. As noted, the "clean" fossil fuel technology was characterized by the high end of the range, which every renewable project competes with. Solar only variations produce LCOW's closer to local market prices at \$2.00-3.21/m^3, however power generation intermittency associated with the solar only infrastructure may make these less desirable. The US offshore wind industry will also miss an opportunity for large scale infrastructure funding, which it needs for future competition with US solar.

Not only do renewables compete with fossil fuel economically, they also provide environmental, ecological and social benefits. By employing renewable energy instead of fossil fuels, 1.7-1,900,000 cars worth of CO2 can be saved. With rising greenhouse gas and global warming levels, it is more important than ever to create new infrastructure with a low carbon footprint. The water withdrawal averted by choosing renewables is another clear environmental benefit. While solar and wind withdraw only ~61,000 m^3/yr, the fossil fuel variations dwarf this with ~27-31,000,000 m^3/yr. Thermal plants, like those examined in this study, often return water to local sources with damaging ecological effects. By using renewables, these negative impacts can be avoided entirely. Finally, renewables showed a substantially greater impact on labor markets, optimistically producing ~108-109,000 jobs to fossil fuel's ~11-1300. Local economies along the border have been heavily stressed by ineffective water management, which has bled into the labor force. By creating sustainable water infrastructure in the region, thousands of skilled jobs can be added to spur economic growth.

Renewable energy is crucial for an environmentally secure future and affirmation that these technologies are cost competitive shows the validity of using them in a project of this scope. While the average US domestic cost of water, ranging from around \$0.27/m^3 to over \$1.87/m^3, remains slightly lower than what the proposed projects can obtain, dynamic selling and purchasing of

power can further reduce the levelized cost of water and is likely to bring the cost into a more satisfactory region. Future iterations of the project that explore optimized pumping, energy storage/sales and more favorable financing may yield rates that can economically compete with locally supplied sources. In doing so, water security along the border can be guaranteed for decades into the future and help develop the region into a more economically active area.

4. CONCLUSION OF STUDIES

Phasing out fossil fuel in favor of renewable energy can reverse the global effects of climate change in a socio-economically favorable manor. Constant innovation actively drives down cost, fueling the argument that renewables are poised to replace their counterparts. Wind turbines are seeing a large portion of this advancement as original designs are rethought in favor of economic benefits. The hydraulic transmission, evaluated in these studies, provides an example of a financially beneficial innovation related to offshore wind turbines. It has been shown that this transmission can reduce the levelized cost of electricity by 3.92-18.8% for offshore wind, which makes renewables even more cost competitive in the fight for sustainability.

Related to the climate change crisis is the ongoing threat of water security experienced by a growing number of regions around the world. Instead of treating these issues as separate events with differing solutions, this collection of studies evaluates how the two may benefit from co-integration in large scale infrastructure. Renewable technology, like the hydraulic wind turbine, is used to provide desalinated water along the US-Mexico border at a levelized cost of $2.20-3.52/m^3. Although expensive compared to locally sourced water, this concept produces and delivers water in a responsible fashion. Renewable powered variations avert adding the equivalent of 1.8-2,100,000 cars worth of CO2 pollution per year, avoid withdrawing the equivalent of 65-75,000 US households worth of water for power generation annually and add potentially over 100,000 more jobs when compared to 27 fossil fuel powered configurations. Regions such as the border are in dire need of sustainable water and co-integration of renewables and desalination will achieve this infrastructure.

REFERENCES

[1] Haigh J. A Brief History of the Earth's CO2. BBC News 2017.

[2] Rice D. Earth's Carbon Dioxide Levels Continue to Soar, At Highest Point in 800,000 Years. USA Today 2018.

[3] Lindsey R. Climate Change: Atmoshperic Carbon Dioxide. NOAA 2020. https://www.climate.gov/news-features/understanding-climate/climate-change-atmospheric-carbon-dioxide.

[4] Plass G. Carbond Dioxide and Climate. Sci Am 2008.

[5] Solomon S, Plattner G-K, Knutti R, Friedlingstein P. Irreversible Climate Change Due to Carbon Dioxide Emissions. PNAS 2009. doi:https://doi.org/10.1073/pnas.0812721106.

[6] N/A. Climate Change on Ecosystems. US Environ Prot Agency n.d. https://archive.epa.gov/epa/climate-impacts/climate-impacts-ecosystems.html#:~:text=Climate change can alter where,wildfires%2C floods%2C and drought.

[7] Ornes S. Core Concept: How Does Climate Change Influence Extreme Weather? Impact Attribution Research Seeks Answers. PNAS 2018. doi:https://doi.org/10.1073/pnas.1811393115.

[8] Lindsey R. Climate Change: Global Sea Level. NOAA 2020. https://www.climate.gov/news-features/understanding-climate/climate-change-global-sea-level.

[9] Brown O. Migration and Climate Change. 2008.

[10] Hauer ME. Sea-level rise and human migration. Nat Rev Earth Environ 2020;1. doi:10.1038/s43017-019-0002-9.

[11] Eickemeier P, Schlömer S, Farahani E, Kadner S, Brunner S, Baum I, et al. Climate Change 2014 Mitigation of Climate Change Working Group III Contribution to the Fifth Assessment Report of the Intergovernmental Panel on Climate Change. 2014.

[12] UNFCCC. Kyoto Protocol Reference Manual. 2008.

[13] United Nations. Paris Agreement. 2015.

[14] International Renewable Energy Agency. Renewable Power Generation Costs in 2019. 2019.

[15] American Wind Energy Association. U.S. Offshore Wind Power Economic Impact Assessment 2020.

[16] Beiter P, Spitsen P, Musial W, Lantz E. The Vineyard Wind Power Purchase Agreement: Insights for Estimating Costs of U.S. Offshore Wind Projects. Natl Renew Energy Lab 2018.

[17] Walter M, Philipp B, Spitsen P, Nunemake J, Gevorgian V. 2018 Offshore Wind Technologies Market Report 2018:1–94.

[18] Mills AD, Millstein D, Jeong S, Lavin L, Wiser R, Bolinger M. Estimating the value of offshore wind along the United States' Eastern Coast. Environ Res Lett 2018;13. doi:10.1088/1748-9326/aada62.

[19] Milborrow D. Global Cost Analysis - The Year Offshore Wind Costs Fell n.d. https://www.windpowermonthly.com/article/1380738/global-costs-analysis-year-offshore-wind-costs-fell.

[20] U.S. Energy Information Administration. Cost and Performance Characteristics of New Generating Technologies. 2019.

[21] Fu R, Feldman D, Margolis R. U.S. Solar Photovoltaic System Cost Benchmark: Q1 2018. Natl Renew Energy Lab 2018:1–47. doi:10.7799/1325002.

[22] Esquivel-Puentes HA, Vacca A, Chamorro LP, Garcia-Bravo JM, Bocanegra Evans H, Doosttalalb A, et al. Energy Harvesting Using Horizontal Axis Wind Turbines With Hydrostatic Transmission. 73rd Annu. Meet. APS Div. Fluid Dyn., 2020.

[23] Shingleton J. One-Axis Trackers – Improved Reliability , Durability , Performance , and Cost Reduction. 2008.

[24] Awasthi A, Shukla AK, Murali Manohar SR, Dondariya C, Shukla KN, Porwal D, et al. Review on sun tracking technology in solar PV system. Energy Reports 2020;6:392–405. doi:10.1016/j.egyr.2020.02.004.

[25] Rodríguez-Gallegos CD, Liu H, Gandhi O, Singh JP, Krishnamurthy V, Kumar A, et al. Global Techno-Economic Performance of Bifacial and Tracking Photovoltaic Systems. Joule 2020;4:1514–41. doi:10.1016/j.joule.2020.05.005.

[26] Laguna AJ. Steady-State Performance of the Delft Offshore Turbine. Delft University of Technology, 2010.

[27] Pusha A, Izadian A, Hamzehlouia S, Girrens N, Anwar S. Modeling of gearless wind power transfer. IECON Proc (Industrial Electron Conf 2011:3176–9. doi:10.1109/IECON.2011.6119818.

[28] Qin C, Innes-Wimsatt E, Loth E. Hydraulic-electric hybrid wind turbines: Tower mass saving and energy storage capacity. Renew Energy 2016;99:69–79. doi:10.1016/j.renene.2016.06.037.

[29] Thomsen KE, Dahlhaug OG, Niss MOK, Haugset SK. Technological advances in hydraulic drive trains for wind turbines. Energy Procedia 2012;24:76–82. doi:10.1016/j.egypro.2012.06.089.

[30] Roggenburg M, Esquivel-Puentes HA, Vacca A, Bocanegra Evans H, Garcia-Bravo JM, Warsinger DM, et al. Techno-economic analysis of a hydraulic transmission for floating offshore wind turbines. Renew Energy 2020;153:1194–204. doi:10.1016/j.renene.2020.02.060.

[31] U.S. Department of Energy Office of Indian Energy Policy and Programs. Levelized Cost of Energy (LCOE). US Dep Energy 2015:9. doi:10.1007/s11096-015-0064-9.

[32] Short W, Packey DJ. A Manual for the Economic Evaluation of Energy Efficiency and Renewable Energy Technologies. 1995.

[33] Lazard. Lazard's Levelized Cost of Energy Analysis - Version 12.0 2018:0–19.

[34] U.S. Energy Information Administration. Levelized Cost and Levelized Avoided Cost of New Generation Resources. Annu Energy Outlook 2019 2019:25.

[35] World Health Organization. Drinking Water 2017. https://www.who.int/news-room/fact-sheets/detail/drinking-water#:~:text=In 2017%2C 71%25 of the,at least a basic service.

[36] Ritchie H, Roser M. Clean Water. Our World Data 2019. https://ourworldindata.org/water-access.

[37] Baker A. What It's Like to Live Through Cape Town's Water Crisis. Time Mag 2019.

[38] Veolia Water Technologies. Desalination Plant. Veolia Water Technol n.d. http://www.veoliawatertechnologies.co.za/water-solutions/desalination/desalination-plant/.

[39] Karthikeyan D, Gupta S. "I'm Scared for my Daughter": Life in India's First City That's Almost Out of Water. CNN 2019.

[40] Water Technology. Minjur Desalination Plant, Tamil Nadu, India. Water Technol n.d. https://www.water-technology.net/projects/minjurdesalination/#:~:text=The Minjur desalination plant is the largest desalination plant in,flocculation%2C gravity and pressure filtration.&text=It is the largest desalination plant in India.

[41] Chennai Metropolitan Water Supply & Sewerage Board. Desalination Plant at Nemmeli n.d.

[42] Kumar M, Culp T, Shen Y. Water Desalination: History, Advances, and Challenges. Front. Eng. Reports Leading-Edge Eng. from 2016 Symp., The National Academies Press; 2017.

[43] United States Geological Survey. Where is Earth's Water? United States Geol Surv n.d. https://www.usgs.gov/special-topic/water-science-school/science/where-earths-water?qt-science_center_objects=0#qt-science_center_objects.

[44] Callegary J., Minjarez Sosa I, Tapia Villasenor E., dos Santos P, Monreal Saavedra R, Grijalva Noriega FJ, et al. Binational study of the transboundary san pedro aquifer: Final Report. Int Bound Water Comm 2016:173.

[45] Sanchez R, Lopez V, Eckstein G. Identifying and characterizing transboundary aquifers along the Mexico-US border: An initial assessment. J Hydrol 2016;535:101–19. doi:10.1016/j.jhydrol.2016.01.070.

[46] Carter NT, Mulligan SP, Seelke CR. U.S.- Mexican Water Sharing : Background and Recent Developments. 2017.

[47] U.S. Environmental Protection Agency. U.S.-Mexico Border Water Infrastructure Program. 2011.

[48] Kitroeff N. "This Is a War": Cross-Border Fight Over Water Erupts in Mexico. New York Times 2020.

[49] International Renewable Energy Agency. Renewable Power Generation Costs in 2017. 2018. doi:10.1007/SpringerReference_7300.

[50] Tadayon S, Tadayon B, Martin D. Wind Turbine Blade System With Air Passageway. US 8449255, 2013.

[51] Gutierrez W, Ruiz-Columbie A, Tutkun M, Castillo L. Impacts of the Low-Level Jet's Negative Wind Shear on the Wind Turbine. Wind Energy Sci Discuss 2017:1–22. doi:10.5194/wes-2017-22.

[52] Carroll J, McDonald A, McMillan D. Failure rate, repair time and unscheduled O&M cost analysis of offshore wind turbines. Wind Energy 2016;19:1107–19. doi:10.1002/we.1887.

[53] Carroll J, McDonald A, Dinwoodie I, McMillan D, Revie M, Lazakis I. Availability, operation and maintenance costs of offshore wind turbines with different drive train configurations. Wind Energy 2017;20:361–78. doi:10.1002/we.2011.

[54] Bhardwaj U, Teixeira AP, Soares CG. Reliability prediction of bearings of an offshore wind turbine gearbox. Adv Renew Energies Offshore - Proc 3rd Int Conf Renew Energies Offshore, RENEW 2018 2019;141:779–87. doi:10.1016/j.renene.2019.03.136.

[55] Kang J, Sun L, Guedes Soares C. Fault Tree Analysis of floating offshore wind turbines. Renew Energy 2019;133:1455–67. doi:10.1016/j.renene.2018.08.097.

[56] Habibi S, Goldenberg A. A Mechatronics Approach for the Design of a New High Performance ElectroHydraulic Actuator. SAE Tech Pap Ser 2010;1. doi:10.4271/1999-01-2853.

[57] Izadian A, Hamzehlouia S, Deldar M, Anwar S. A hydraulic wind power transfer system: Operation and modeling. IEEE Trans Sustain Energy 2014;5:457–65. doi:10.1109/TSTE.2013.2291835.

[58] Skaare B, B. Hörnsten, Nielsen FG. Modeling, simulation and control of a wind turbine with a hydraulic transmission system. Wind Energy 2015;18:1875–91. doi:10.1002/we.

[59] Jiang Z, Yang L, Gao Z, Moan T. Numerical simulation of a wind turbine with a hydraulic transmission system. Energy Procedia 2014;53:44–55. doi:10.1016/j.egypro.2014.07.214.

[60] Jarquin-Laguna A. Simulation of an offshore wind farm using fluid power for centralized electricity generation. J Phys Conf Ser 2016;753. doi:10.1088/1742-6596/753/10/102004.

[61] Hamzehlouia S, Izadian A, Pusha A, Anwar S. Controls of hydraulic wind power transfer. IECON Proc (Industrial Electron Conf 2011:2475–80. doi:10.1109/IECON.2011.6119698.

[62] Izadian A. Central Wind Turbine Power Generation. PCT/US2010/061972, n.d.

[63] Hamzehlouia S, Izadian A. Modeling of hydraulic wind power transfers. 2012 IEEE Power Energy Conf Illinois, PECI 2012 2012:1–6. doi:10.1109/PECI.2012.6184610.

[64] Tao J, Wang H, Liao H, Yu S. Mechanical design and numerical simulation of digital-displacement radial piston pump for multi-megawatt wind turbine drivetrain. Renew Energy 2019;143:995–1009. doi:10.1016/j.renene.2019.04.159.

[65] Wang F, Chen J, Xu B, Stelson KA. Improving the reliability and energy production of large wind turbine with a digital hydrostatic drivetrain. Appl Energy 2019;251:113309. doi:10.1016/j.apenergy.2019.113309.

[66] Yin X xing, Lin Y gang, Li W, Gu H gang. Hydro-viscous transmission based maximum power extraction control for continuously variable speed wind turbine with enhanced efficiency. Renew Energy 2016;87:646–55. doi:10.1016/j.renene.2015.10.032.

[67] Rajabhandharaks D. Control of Hydrostatic Transmission Wind Turbine. San Jose State University, 2014.

[68] Power AI. A Fully-Variable Transmission Designed to Survive n.d. http://www.artemisip.com/sectors/renewables/.

[69] Windera Power Systems. Introducing the Windera System n.d. http://www.winderapowersystems.com/.

[70] Caldwell NJ. Digital Displacement Hydrostatic Transmission Systems. The University of Edinburgh, 2007.

[71] Fingersh L, Hand M, Laxson A. NREL Wind Turbine Design Cost and Scaling Model. 2006. doi:10.2172/897434.

[72] Carlin PW, Laxson a S. The History and State of the Art of Variable-Speed Wind Turbine Technology The History and State of the Art of Variable-Speed Wind Turbine Technology 2001.

[73] Yin X xing, Lin Y gang, Li W, Liu H wei, Gu Y jing. Output power control for hydro-viscous transmission based continuously variable speed wind turbine. Renew Energy 2014;72:395–405. doi:10.1016/j.renene.2014.07.010.

[74] Dasgupta K. Analysis of a hydrostatic transmission system using low speed high torque motor. Mech Mach Theory 2000;35:1481–99. doi:10.1016/S0094-114X(00)00005-7.

[75] Akkaya AV. Effect of bulk modulus on performance of a hydrostatic transmission control system. Sadhana - Acad Proc Eng Sci 2006;31:543–56. doi:10.1007/BF02715913.

[76] Bobrow JE, Sohl GA. Experiments and simulations on the nonlinear control of a hydraulic servosystem. IEEE Trans Control Syst Technol 1999;7:238–47. doi:10.1109/87.748150.

[77] Radial piston hydraulic motor: Hägglunds CBm 2012.

[78] Moné C, Hand M, Bolinger M, Rand J, Heimiller D, Ho J. NREL 2015 Cost of Wind Energy Review 2015. doi:NREL/TP-5000-52920.

[79] G. Saur, B. Maples, B. Meadows, M. Hand, W. Musial, C. Elkinton JC. NREL Offshore Wind Plant Balance-of-Station Cost Drivers and Sensitivities 2012:56132.

[80] Maness M, Maples B, Smith A. NREL Offshore Balance-of-System Model 2017.

[81] Bosch-Rexroth Group n.d.

[82] Desmond C, Murphy J, Blonk L, Haans W. Description of an 8 MW reference wind turbine. J Phys Conf Ser 2016;753. doi:10.1088/1742-6596/753/9/092013.

[83] Rodrigues S, Restrepo C, Katsouris G, Pinto RT, Soleimanzadeh M, Bosman P, et al. A Multi-Objective Optimization Framework For Offshore Wind Farm Layouts And Electric Infrastructures. Energies 2016;9:1–42. doi:10.3390/en9030216.

[84] Gifford JS, Grace RC. NREL Cost of Renewable Energy Spreadsheet Tool (CREST): A Model for Developing Cost-Based Incentives in the United States, User Manual Version 4 2013:1–36.

[85] Bailey H, Brookes KL, Thompson PM. Assessing environmental impacts of offshore wind farms: Lessons learned and recommendations for the future. Aquat Biosyst 2014;10:1–13. doi:10.1186/2046-9063-10-8.

[86] Miedema R. Offshore Wind Energy Operations and Maintenance Analysis 2012:0–83.

[87] Buck BH, Langan R. Aquaculture perspective of multi-use sites in the open ocean: The untapped potential for marine resources in the anthropocene. Aquac Perspect Multi-Use Sites Open Ocean Untapped Potential Mar Resour Anthr 2017:1–404. doi:10.1007/978-3-319-51159-7.

[88] Martin R, Lazakis I, Barbouchi S, Johanning L. Sensitivity analysis of offshore wind farm operation and maintenance cost and availability. Renew Energy 2016;85:1226–36. doi:10.1016/j.renene.2015.07.078.

[89] N/A. NREL Annual Technology Baseline 2018 n.d. https://atb.nrel.gov/electricity/2018/index.html?t=ow.

[90] Capacity Factors at Danish Offshore Wind Farms n.d. http://energynumbers.info/capacity-factors-at-danish-offshore-wind-farms.

[91] Lantz E, Leventhal M, Baring-Gould I. Wind Power Project Repowering: Financial Feasibility, Decision Drivers, and Supply Chain Effects 2013. doi:10.2172/1117058.

[92] Distributed Generation Energy Project Financing - USDA Rural Development n.d. https://www.rd.usda.gov/programs-services/distributed-generation-energy-project-financing.

[93] U.S. Energy Information Administration. Electric Power Monthly: with data for May 2014 2014:1–222.

[94] U.S. Energy Information Administration. January 2019 Monthly Energy Review. vol. 0035. 2019.

[95] Kirby BJ, Ridge O, Dyer J, Martinez C, Group EP. Frequency Control Concerns In The North American Electric Power System. 2002.

[96] Obaid ZA, Cipcigan LM, Abrahim L, Muhssin MT. Frequency control of future power systems: reviewing and evaluating challenges and new control methods. J Mod Power Syst Clean Energy 2019;7:9–25. doi:10.1007/s40565-018-0441-1.

[97] Oh KY, Nam W, Ryu MS, Kim JY, Epureanu BI. A review of foundations of offshore wind energy convertors: Current status and future perspectives. Renew Sustain Energy Rev 2018;88:16–36. doi:10.1016/j.rser.2018.02.005.

[98] Wu X, Hu Y, Li Y, Yang J, Duan L, Wang T, et al. Foundations of offshore wind turbines: A review. Renew Sustain Energy Rev 2019;104:379–93. doi:10.1016/j.rser.2019.01.012.

[99] O'Kelly BC, Arshad M. Offshore wind turbine foundations - analysis and design. Elsevier Ltd; 2016. doi:10.1016/B978-0-08-100779-2.00020-9.

[100] Lips M. Length of Operational Life and Its Impact on Life-Cycle Costs of a Tractor in Switzerland. Agriculture 2017;7:68. doi:10.3390/agriculture7080068.

[101] GUO S, CHEN J, LU Y, WANG Y, DONG H. Hydraulic piston pump in civil aircraft: Current status, future directions and critical technologies. Chinese J Aeronaut 2019. doi:10.1016/j.cja.2019.01.013.

[102] Fischetti M. Bold Plan? Replace the Border Wall with an Energy–Water Corridor. Sci Am 2019.

[103] Castillo L, George WK, Gore J, Adrian R, Bocanegra Evans H, Gutierrez W, et al. An Energy-Water Corridor Along the US/Mexico Border: Changing the Conversation. 2019.

[104] Ahmed A. The Engineers' Plan for Creating Border Security With Clean Energy. Atl 2019.

[105] U.S. Census Buraeu. Top Trading Partners - &cm 2020 n.d. https://www.census.gov/foreign-trade/statistics/highlights/toppartners.html.

[106] Carter NT, Mulligan SP, Stern C V. Sharing the Colorado River and the Rio Grande : Cooperation and Conflict with Mexico. 2018.

[107] Konikow LF. Groundwater Depletion in the United States (1900-2008). US Dep Inter US Geol Surv 2013. doi:10.1016/0969-806x(93)90261-r.

[108] United States Geological Survey. US Aquifer Summary. US Dep Inter n.d.

[109] United States Geological Survey. National Water Information - 2016 2016. doi:http://dx.doi.org/10.5066/FP55KJN.

[110] Bunch S, Cort K, Johnson E, Elliot D, McMordie-Stoughton K. Water and Wastewater Annual Price Escalation Rates for Selected Cities across the United States. 2017. doi:DOW/EE.1670.

[111] Kim J, Park K, Yang DR, Hong S. A comprehensive review of energy consumption of seawater reverse osmosis desalination plants. Appl Energy 2019;254. doi:10.1016/j.apenergy.2019.113652.

[112] Cresko J, Rao P, Aghajanzadeh A, Sheaffer P, Morrow WR, Dollinger C, et al. Bandwidth Study on Energy Use and Potential Energy Savings Opportunities in U.S. Seawater Desalination Systems. Dep Energy 2017.

[113] Shatat M, Riffat S, Ghabayen S. State of Art Water Desalination Technologies Using Conventional and Sustainable Energy Sources. 4th Int Eng Conf –Towards Eng 21st Century 2012.

[114] National Research Council. Desalination: A National Perspective. 2008.

[115] American Membrane Technology Association. Seawater Desalination Costs. 2012.

[116] Kim YM, Kim SJ, Kim YS, Lee S, Kim IS, Kim JH. Overview of systems engineering approaches for a large-scale seawater desalination plant with a reverse osmosis network. Desalination 2009;238:312–32. doi:10.1016/j.desal.2008.10.004.

[117] Swaminathan J, McGovern RK, Chung H-W, Warsinger DM, Lienhard JH. Multi-Effect Membrane Distillation. 10392270, 2019.

[118] Jacobsen R. Israel Proves the Desalination Era Is Here. Sci Am 2016.

[119] Water Technology. Sorek Desalination Plant. Water Technol n.d. https://www.water-technology.net/projects/sorek-desalination-plant/.

[120] Fountain H. The World Can Make More Water From The Sea, But At What Cost? New York Times 2019.

[121] Beiter P, Musial W, Kilcher L, Maness M, Smith A. An Assessment of the Economic Potential of Offshore Wind in the United States from 2015 to 2030. Natl Renew Energy Lab 2017. doi:10.2172/1349721.

[122] Schwartz M, Heimiller D, Haymes S, Musial W. Assessment of Offshore Wind Energy Resources for the United States. 2010.

[123] Musial W, Butterfield S. Future for Offshore Wind Energy in the United States. 2004.

[124] Musial W, Ram B. Large-Scale Offshore Wind Power in the United States - National Renewable Energy Laboratory. 2010. doi:10.2172/990101.

[125] Mazzeo D, Matera N, Luca P De, Baglivo C, Maria P, Oliveti G. Worldwide geographical mapping and optimization of stand-alone and grid- connected hybrid renewable system techno-economic performance across Köppen-Geiger climates. Appl Energy 2020;276:115507. doi:10.1016/j.apenergy.2020.115507.

[126] U.S. Department of Energy. Solar Energy Potential n.d. https://www.energy.gov/maps/solar-energy-potential.

[127] Renné D, George R, Wilcox S, Stoffel T, Myers D, Heimiller D. Solar Resource Assessment. 2008.

[128] Leitner A, Owens B. Brighter than a Hundred Suns: Solar Power for the Southwest 2003.

[129] Southwestern States Have Better Solar Resources and Higher Solar PV Capacity Factors 2019. https://www.eia.gov/todayinenergy/detail.php?id=39832.

[130] International Renewable Energy Agency. Renewable Power Generation Costs in 2018. 2018. doi:10.1007/SpringerReference_7300.

[131] H J Editorial Team. The Mega-ton Water System. Sci Technol 2013.

[132] United States Geological Survey. SRTM 1 Arc-Second Global 2015. doi:/10.5066/F7PR7TFT.

[133] Draxl C, Hodge B-M, Clifton A, Mccaa J. Overview and Meteorological Validation of the Wind Integration National Dataset Toolkit. 2015.

[134] Draxl C, Nrel AC. A Guide to Using the WIND Toolkit Validation Code A Guide to Using the WIND Toolkit Validation Code. 2014.

[135] King J, Clifton A, Hodge B, King J. Validation of Power Output for the WIND Toolkit Validation of Power Output for the WIND Toolkit. 2014.

[136] Draxl C, Clifton A, Hodge BM, McCaa J. The Wind Integration National Dataset (WIND) Toolkit. Appl Energy 2015;151:355–66. doi:10.1016/j.apenergy.2015.03.121.

[137] Sengupta M, Xie Y, Lopez A, Habte A, Maclaurin G, Shelby J. The National Solar Radiation Data Base (NSRDB). Renew Sustain Energy Rev 2018;89:51–60. doi:10.1016/j.rser.2018.03.003.

[138] Duffie JA, Beckman WA. Solar Engineering of Thermal Processes. vol. 53. 2013. doi:10.1119/1.14178.

[139] Castillo L, Gutierrez W, Gore J. Renewable Energy Saves Water and Creates Jobs. Sci Am 2018.

[140] Stern C V. Drought Contingency Plans for the Colorado River Basin. vol. 2019. 2019.

[141] Ren Y, Wei S, Cheng K, Fu Q. Valuation and pricing of agricultural irrigation water based on macro and micro scales. Water (Switzerland) 2018;10:1–13. doi:10.3390/w10081044.

[142] N/A. Water Use and Pricing in Agriculture 1993:45–57.

[143] Wichelns D. Agricultural Water Pricing: United States. 2010.

[144] N/A. Reservoir Design and Storage Volume. Water Syst. Des. Man., vol. I, 2001, p. 1–18.

[145] Calise F, Cappiello FL, Vanoli R, Vicidomini M. Economic assessment of renewable energy systems integrating photovoltaic panels , seawater desalination and water storage. Appl Energy 2019;253:113575. doi:10.1016/j.apenergy.2019.113575.

[146] Dol AW, Chalise R, Hadjerioua B, Manwaring M, Bishop N. Development and Implications of a Predictive Cost Methodology for Modular Pumped Storage Hydropower (m-PSH) Projects in the United States. 2016. doi:10.13140/RG.2.2.10441.54881.

[147] National Hydropower Association. 2018 Pumped Storage Report. 2018.

[148] National Hydropower Association. Challenges and Opportunities For New Pumped Storage Development 2013;6:33.

[149] Swamee PK, Jain AK. Explicit Equations for Pipe-Flow Problems. ASCE J Hydraul Div 1976;102:657–64.

[150] Clark RM, Sethi V, Selvakumar A. Cost Models for Water Supply Distribution Systems. J Water Resour Planin Manag 2002;9496. doi:10.1061/(ASCE)0733-9496(2002)128.

[151] N/A. Roughness & Surface Coefficients. Eng Toolbox 2003. https://www.engineeringtoolbox.com/surface-roughness-ventilation-ducts-d_209.html.

[152] N/A. Maximum Flow Velocities in Water Systems. Eng Toolbox 2003. https://www.engineeringtoolbox.com/flow-velocity-water-pipes-d_385.html.

[153] Voutchkov N. Desalination Engineering Planning and Design. McGraw Hill; 2013.

[154] Cordoba SP, Warsinger DM. Split-recovery reverse osmosis for demand response and higher energy efficiency. Under Rev 2020.

[155] Guirguis MJ. Energy Recovery Devices In Seawater Reverse Osmosis Desalination Plants With Emphasis On Efficiency And Economical Analysis Of Isobaric Versus Centrifugal Devices. 2011.

[156] Liberman B. The importance of energy recovery devices in reverse osmosis desalination Desalination Plant Power Demand in Conjunction with Regional Power Demand Infrastructure Leveling the Power Demand. n.d.

[157] Lenntech. Reverse Osmosis Desalination Process n.d. https://www.lenntech.com/processes/desalination/reverse-osmosis/general/reverse-osmosis-desalination-process.htm.

[158] Warsinger DM, Tow EW, Nayar KG, Maswadeh LA, Lienhard V JH. Energy efficiency of batch and semi-batch (CCRO) reverse osmosis desalination. Water Res 2016;106:272–82. doi:10.1016/j.watres.2016.09.029.

[159] Lee T, Rahardianto A, Cohen Y. Multi-cycle operation of semi-batch reverse osmosis (SBRO) desalination. J Memb Sci 2019;588. doi:10.1016/j.memsci.2019.05.015.

[160] Cordoba SP, Das A, Warsinger DM. Improved Batch Reverse Osmosis Configuration for Better Energy Effiency. IDA 2019 World Congr. Water Reuse Desalin., 2019.

[161] Cordoba SP, Das A, Leon J, Garcia J, Warsinger DM. Double-acting batch reverse osmosis configuration for best-in-class efficiency and low downtime. Under Rev 2020.

[162] Warsinger DM, Lienhard JH, Tow EW, McGovern RK, Thiel GP. Batch Pressure-Driven Membrane Separation with Closed-Flow Loop and reservoir. US 2019/0160431, 2019.

[163] Das A, Warsinger DM. Batch Counter-Flow Reverse Osmosis. Desalin (Under Rev 2020.

[164] Nejati S, Mirbagheri SA, Warsinger DM, Fazeli M. Biofouling in seawater reverse osmosis (SWRO): Impact of module geometry and mitigation with ultrafiltration. J Water Process Eng 2019;29. doi:10.1016/j.jwpe.2019.100782.

[165] Jiang S, Li Y, Ladewig BP. A review of reverse osmosis membrane fouling and control strategies. Sci Total Environ 2017;595:567–83. doi:10.1016/j.scitotenv.2017.03.235.

[166] Missimer TM, Maliva RG. Environmental issues in seawater reverse osmosis desalination: Intakes and outfalls. Desalination 2018;434:198–215. doi:10.1016/j.desal.2017.07.012.

[167] Petersen KL, Heck N, Reguero BG, Potts D, Hovagimian A, Paytan A. Biological and physical effects of brine discharge from the Carlsbad Desalination plant and implications for future desalination plant constructions. Water (Switzerland) 2019;11. doi:10.3390/w11020208.

[168] Musial W, Beiter P, Schwabe P, Tian T, Stehly T, Spitsen P. 2016 Offshore Wind Technologies Market Report. 2016.

[169] Anaya-Lara O, Tande JO, Uhlen K, Merz K, Anaya-Lara O, Tande JO. Offshore Transmission Technology. Offshore Wind Energy Technol 2018;2011:345–79. doi:10.1002/9781119097808.ch9.

[170] Stewart G, Muskulus M. A Review and Comparison of Floating Offshore Wind Turbine Model Experiments. Energy Procedia 2016;94:227–31. doi:10.1016/j.egypro.2016.09.228.

[171] NOAA National Geophysical Data Center. U.S. Coastal Relief Model Vol.6 - Southern California 2003. doi:10.7289/V500001J.

[172] NOAA National Geophysical Data Center. U.S. Coastal Relief Model Vol.5 - Western Gulf of Mexico 2001. doi:10.7289/V5QJ7F79.

[173] Energy Technology Systems Analysis Programme. Electricity Transmission and Distribution. 2014. doi:10.1109/melcon.1996.550955.

[174] U.S. Energy Information Administration. Assessing HVDC Transmission for Impacts of Non - Dispatchable Generation. 2018.

[175] Xiang X, Merlin MMC, Green TC. Cost analysis and comparison of HVAC, LFAC and HVDC for offshore wind power connection. IET Conf Publ 2016;2016:1–6. doi:10.1049/cp.2016.0386.

[176] Andrade J, Baldick R. Estimation of Transmission Costs for New Generation. 2017.

[177] University of Michigan Center For Sustainable Systems. Wind Energy Factsheet. 13th Ger Wind Energy Conf 2017;10:1–158. doi:10.1016/B978-0-12-804448-3/00004-9.

[178] Hofmann M, Sperstad IB. Will 10 MW wind turbines bring down the operation and maintenance cost of offshore wind farms? Energy Procedia 2014;53:231–8. doi:10.1016/j.egypro.2014.07.232.

[179] General Electric. Haliade-X 12 MW offshore wind platform n.d. https://www.ge.com/renewableenergy/wind-energy/offshore-wind/haliade-x-offshore-turbine.

[180] Bortolotti P, Canet Tarres H, Dykes K, Merz K, Sethuraman L, Verelst D, et al. Systems Engineering in Wind Energy - WP2.1 Reference Wind Turbines. 2019.

[181] Reindl DT, Beckman WA, Duffie JA. Diffuse fraction correlations. Sol Energy 1990;45:1–7. doi:10.1016/0038-092X(90)90060-P.

[182] Dervishi S, Mahdavi A. Computing diffuse fraction of global horizontal solar radiation: A model comparison. Sol Energy 2012;86:1796–802. doi:10.1016/j.solener.2012.03.008.

[183] Erbs DG, Klein SA, Duffie JA. Estimation of the diffuse radiation fraction for hourly, daily and monthly-average global radiation. Sol Energy 1982;28:293–302. doi:10.1016/0038-092X(82)90302-4.

[184] Buzoianu M, Brockwell A, Seppi D. A dynamic supply-demand model for electricity prices 2005.

[185] Dutta G, Mitra K. A literature review on dynamic pricing of electricity. J Oper Res Soc 2017;68:1131–45. doi:10.1057/s41274-016-0149-4.

[186] Stehly T, Beiter P. NREL 2018 Cost of Wind Energy Review. 2019.

[187] U.S. Energy Information Administration. Electric Power Monthly with Data for June 2020. 2020.

[188] Pletka R, Khangura J, Rawlines A, Waldren E, Wilson D. Capital Costs for Transmission and Substations. 2014.

[189] Connor PWO, Fen Q, Zhang K, Deneale ST. Hydropower Baseline Cost Modeling. 2015.

[190] Petheram C, McMahon TA. Dams, dam costs and damnable cost overruns. J Hydrol X 2019;3:100026. doi:10.1016/j.hydroa.2019.100026.

[191] Musial W, Beiter P, Nunemaker J. Cost of Floating Offshore Wind Energy Using New England Aqua Ventus Concrete Semisubmersible Technology 2020:43.

[192] International Renewable Energy Agency. The Power to Change: Solar and Wind Cost Reduction Potential to 2025. 2016.

[193] U.S. Environmental Protection Agency. Inventory of U.S. Greenhouse Gas Emissions and Sinks. n.d.

[194] O'Donoughue P, Heath G, Dolan SL, Vorum M. Life Cycle Greenhouse Gas Emissions of Electricity Generated from Conventionally Produced Natural Gas. J Ind Ecol 2014. doi:https://doi.org/10.1111/jiec.12084.

[195] Heath GA, Donoughue PO, Arent DJ, Bazilian M. Harmonization of initial estimates of shale gas life cycle greenhouse gas emissions for electric power generation 2014. doi:10.1073/pnas.1309334111.

[196] National Renewable Energy Laboratory. Wind LCA Harmonization. 2013. doi:10.1111/j.1530-9290.2012.00464.x/pdf.National.

[197] Heath G, Sandor D. Life Cycle Greenhouse Gas Emissions from Solar Photovoltaics 2012.

[198] National Renewable Energy Laboratory. Life Cycle Greenhouse Gas Emissions from Electricity Generation. 2013.

[199] U.S. Department of Energy. Renewable Energy & Energy Efficiency Projects - Loan Guatantee Solicitation. 2014.

[200] Monnin P. The Impact of Interest Rates on Electricity Production Costs. 2015.

[201] Rao AK, Li OR, Wrede L, Elias C, Cordoba S, Roggenburg M, et al. A Framework for Blue Energy Generation via Reverse Osmosis. Nat Sustain (Under Rev 2020.

[202] Gao Y, Gao X, Zhang X. The 2 ° C Global Temperature Target and the Evolution of the Long-Term Goal of Addressing Climate Change — From the United Nations Framework Convention on Climate Change to the Paris Agreement. Engineering 2017;3:272–8. doi:10.1016/J.ENG.2017.01.022.

[203] U.S. Environmental Protection Agency. Greenhouse Gas Emissions from a Typical Passenger Vehicle. 2018.

[204] U.S. Environmental Protection Agency. How We Use Water n.d. https://www.epa.gov/watersense/how-we-use-water#:~:text=Water in Daily Life,-In the US&text=The average American family uses,in more water-intensive landscapes.

[205] Sunpower. 430 – 450 W Commercial A-Series Panels 2019.

APPENDIX A. WIND ENERGY PRODUCTION MODELING:

Table A-1: A list of design parameters for the modeled project turbine[180].

Turbine Parameters	
Rated Capacity (MW)	10
Cut-in Speed (m/s)	4
Cut-out Speed (m/s)	25
Rated Speed (m/s)	11
Hub Height (m)	119
Blade Length (m)	98
Generator Efficiency (%)	94.4

The instantaneous turbine power output profile (P_T) is modelled at a given wind speed as shown in Equation A-1, with rated power (P_R), wind velocity (V_W), cut-in velocity (V_{in}) and rated velocity (V_R):

$$P_T = P_R * \left(\frac{V_W^n - V_{in}^n}{V_R^n - V_{in}^n}\right) \quad \text{(A-1)}$$

The coefficient of power (C_P) is modeled by (A-2) with respect to the power output (P_T), wind velocity (V_W), rotor diameter (A_{rotor}) and air density (ρ_{air}).

$$C_P = P_T \frac{2}{V_w^3 A_{rotor} \rho_{air}} \quad \text{(A-2)}$$

Shape parameters (C) and (k) for weekly-daily Weibull distributions are modeled for the two offshore wind sites using the system of equations A-3,4 with average wind velocity ($\overline{V_W}$) and standard deviation $\left(\overline{Std_{dev}}\right)$, where ($\Gamma$) indicates the Gamma distribution:

$$\overline{V_W} = C\Gamma(1 + \tfrac{1}{\mathrm{k}}) \quad \text{(A-3)}$$

$$\overline{Std_{dev}} = \sqrt{\overline{V_W}^2 \left(\frac{\Gamma\left(1+\frac{2}{k}\right)}{\Gamma^2\left(1+\frac{1}{k}\right)} - 1\right)} \quad \text{(A-4)}$$

Weibull distributions for each site are then resolved using Equation A-5, where (V_w) is the predicted wind speed:

$$Prob_W = \frac{k}{c}\left(\frac{V_W}{c}\right)^{k-1} e^{-\left(\frac{V_W}{c}\right)^k} \quad \text{(A-5)}$$

APPENDIX B. SOLAR ENERGY PRODUCTION MODELING:

Table B-1: Operating parameters for a 450W SunPower solar panel[205].

Panel Properties	Properties
Rated Power (W)	450
Rated Voltage (V)	44.0
Rated Current (A)	10.2
Power Temp Coeff. (%/C)	-0.29
Length (m)	1.999
Width (m)	1.016

The total radiation on the panel is estimated using a model for extraterrestrial radiation on a tiled surface (Eq. B-1). Tracking panel incidence angle (θ_{inc}) and surface tilt (β_{track}) are modeled over the course of a given day using solar declination (δ), solar hour angle (ω), solar zenith angle (θ_z) and solar azimuth angle (γ) according to Equation B-1,2:

$$\theta_{inc} = \arccos\left(\sqrt{(1 - cos^2(\delta))\, sin^2(\omega)}\right) \tag{B-1}$$

$$\beta_{track} = \arctan\left(\tan\left(\theta_z\right)|\cos\left(\gamma_s\right)|\right. \tag{B-2}$$

Cell efficiencies are calculated as a function of temperature by solving a system of Equations B-3,4,5 using the cell reference temperature ($T_{a,ref}$), standard test radiation ($G_{T,ref}$) of 800 W/m^2, the assumed nominal operating cell temperature (*NOCT*) of 45 C, heat transfer coefficient ($\tau\alpha/U$), panel power temperature coefficient (β_{PV}), ambient temperature (T_a), actual cell temperature (T_c), reference efficiency (η_{ref}), maximum power point tracking efficiency (η_{MPPT}) which is assumed to be 0.92 and temperature/MPPT adjusted efficiency (η_{adj})

$$NOCT = T_{a,ref} + G_{T,ref}\frac{\tau\alpha}{U} \tag{B-3}$$

$$T_c - T_a = I_T\frac{\tau\alpha}{U}(1 - \eta_{adj}) \tag{B-4}$$

$$\eta_{adj} = \eta_{MPPT}\eta_{ref}(1 + \beta_{PV}(T_c - T_{c,ref})) \tag{B-5}$$